0026-895X/02/6202-234–249$7.00
MOLECULAR PHARMACOLOGY
Copyright © 2002 The American Society for Pharmacology and Experimental Therapeutics
Mol Pharmacol 62:234–249, 2002

Vol. 62, No. 2
1612/994520
Printed in U.S.A.

The Zebrafish (*Danio rerio*) Aryl Hydrocarbon Receptor Type 1 Is a Novel Vertebrate Receptor

ERIC A. ANDREASEN, MARK E. HAHN, WARREN HEIDEMAN, RICHARD E. PETERSON, and ROBERT L. TANGUAY

Environmental Toxicology Center (E.A.A., W.H., R.E.P.) and School of Pharmacy (W.H., R.E.P.), University of Wisconsin, Madison, Wisconsin; Biology Department (M.E.H.), Woods Hole Oceanographic Institution, Woods Hole, Massachusetts; and Department of Pharmaceutical Sciences (R.L.T.), School of Pharmacy, University of Colorado Health Sciences Center, Denver, Colorado

Received January 16, 2002; accepted April 12, 2002

This article is available online at http://molpharm.aspetjournals.org

ABSTRACT

Fish are known to have two distinct classes of aryl hydrocarbon receptors, and their roles in mediating xenobiotic toxicity remain unclear. In this study, we have identified and characterized a cDNA tentatively named zebrafish *AHR1* (zfAHR1). Analysis of the deduced amino acid sequence reveals that the protein is distinct from zfAHR2 and is more closely related to the mammalian aryl hydrocarbon receptor (AHR). zfAHR1 and zfAHR2 share 40% amino acid identity overall and 58% in the N-terminal half. The z*fAHR1* gene maps to linkage group 16 in a region that shares conserved synteny with human chromosome 7 containing the human *AHR*, suggesting that the *zfAHR1* is the ortholog of the human *AHR. zfAHR2* maps to a separate linkage group (LG22). Both zfAHR mRNAs are expressed in early development, but they are differentially expressed in adult tissues. zfAHR2 can dimerize with zfARNT2b and binds with specificity to dioxin-responsive elements (DREs). Under identical conditions, zfAHR1/zfARNT2b/DRE complexes are formed; however, the interactions are considerably weaker. In COS-7 cells expressing zfARNT2b and zfAHR2, 2,3,7,8-tetrachlorodibenzo-*p*-dioxin (TCDD) exposure leads to a significant induction of dioxin-responsive reporter genes. In identical experiments, TCDD exposure fails to induce the reporter gene in zfAHR1-expressing cells. Ligand-binding experiments suggested that the differential zfAHR activities are attributable to differences in TCDD binding because only zfAHR2 exhibits high-affinity binding to [^{3}H]TCDD or β-naphthoflavone. Finally, using chimeric zfAHR1/zfAHR2 constructs, the lack of TCDD-mediated transcriptional activity was localized to the ligand-binding and C-terminal domains of zfAHR1.

The aryl hydrocarbon receptor (AHR) is a member of the basic helix-loop-helix PAS family of proteins. Members of this family include the aryl hydrocarbon receptor nuclear translocators (ARNT, ARNT2, and ARNT3), hypoxia-inducible factor 1α, *Drosophila melanogaster* single-minded, *D. melanogaster* period, Clock, and others. These proteins are involved in mediating responses to environmental contaminants, low oxygen tension and glucose, circadian rhythm, and various other cues (for review, see Gu et al., 2000). The basic components of the AHR signal transduction pathway are well understood (for review, see Schmidt and Bradfield, 1996). The cytosolic AHR is complexed with at least three chaperone proteins, two molecules of HSP90 and the aryl hydrocarbon interacting protein (AIP, also known as ARA9 or XAP2), enabling proper conformation for ligand binding. Once bound by ligands such as 2,3,7,8-tetrachlorodibenzo-*p*-dioxin (TCDD), the cytosolic AHR translocates to the nucleus, dissociates from the chaperone proteins, and dimerizes with ARNT. This heterodimeric AHR/ARNT complex associates with specific DNA sequences termed dioxin-response elements (DRE, alternatively known as xenobiotic response el-

This work was supported in part by National Institute of Environmental Health Sciences grants ES10820 (to R.L.T.) and ES06272 (to M.E.H.), by National Institute of Environmental Health Sciences Developmental and Molecular Toxicology Center grant P30-ES09090 (to W.H. and R.E.P.), and by the University of Wisconsin Sea Grant Institute under grants from the National Sea Grant College Program, National Oceanic and Atmospheric Administration, United States Department of Commerce, Sea Grant Projects R/BT12 and R/BT 14 (to W.H. and R.E.P.). This is contribution 340 of the University of Wisconsin Environmental Toxicology Center and contribution 10,571 from the Woods Hole Oceanographic Institution.

ABBREVIATIONS: AHR, aryl hydrocarbon receptor; PAS, PER/ARNT/SIM (period/aryl hydrocarbon receptor nuclear translocator/single-minded); ARNT, aryl hydrocarbon nuclear translocator; HSP90, 90-kDa heat shock protein; AIP, aryl hydrocarbon interacting protein; TCDD, 2,3,7,8-tetrachlorodibenzo-*p*-dioxin; DRE, dioxin-responsive element; bHLH, basic helix loop helix; LBD, ligand-binding domain; NLS, nuclear localization; NES, nuclear export; TBDD, 2,3,7,8-tetrabromodibenzo-*p*-dioxin; PCB126, 3,3′,4,4′,5-pentachlorobiphenyl; TCDF, 2,3,7,8-tetrachlorodibenzofuran; PeCDF, 2,3,4,7,8-pentachlorodibenzofuran; BaP, benzo[*a*]pyrene; I3C, indole-3-carbinol; 3MC, 3-methylcholanthrene; I3AA, indole-3-acetic acid; DMBA, 7,12-dimethylbenz[*a*]anthracene; BNF, β-naphthoflavone; PC, phosphatidylcholine; PCR, polymerase chain reaction; hpf, hours postfertilization; TNT, transcription and translation; MOPS, 4-morpholinepropanesulfonic acid; PAGE, polyacrylamide gel electrophoresis; DTT, dithiothreitol; TBS-T, Tris-buffered saline-Tween 20; DMSO, dimethyl sulfoxide; ANOVA, analysis of variance; zf, zebrafish; AHRR, aryl hydrocarbon receptor repressor; RACE, rapid amplification of cDNA ends; CMV, cytomegalovirus; kb, kilobase(s); Fh, *F. heteroclitus.*

ements), altering expression of downstream genes such as cytochrome P4501A1 (for review, see Schmidt and Bradfield, 1996). The expression and ligand activation of the AHR seem to be essential for the manifestation of much of TCDD developmental toxicity, because AHR null mice exhibit few signs of TCDD toxicity (Mimura et al., 1997).

Several laboratories have focused on mapping the functional domains of the AHR (for review, see Fukunaga et al., 1995). The N-terminal fragment of AHR contains the bHLH and PAS domains, which are responsible for DNA binding, and the HLH and PAS domains are involved in dimerization with ARNT [described in Fukunaga et al. (1995)]. The ligand-binding domain (LBD) covers the PAS-B domain, whereas the HSP90 interacts with the bHLH and PAS domains. AIP interacts with the PAS and ligand-binding domains (Meyer and Perdew, 1999). Nuclear localization (NLS) and export (NES) domains have been localized to the bHLH domain (Ikuta et al., 1998). Finally, the transactivation domain was mapped to the C terminus of the AHR (Fukunaga et al., 1995).

Zebrafish (*Danio rerio*) are fast becoming an extremely useful model for studying vertebrate developmental toxicology. Efforts to sequence the zebrafish genome by 2003 will allow perturbations in gene expression to be investigated very rapidly. Theories of the origin of toxicant-induced developmental abnormalities can be tested rapidly because of the vast knowledge of normal development in zebrafish. In addition, mutant screens can be used to study molecular mechanisms for the production of certain signs of toxicity. Efforts to understand the molecular mechanism of TCDD developmental toxicity in fish have lead to the characterization of the AHR pathway in zebrafish. The AHR signal transduction pathway in zebrafish is generally similar to that of mammals, with one notable exception. Fish, including zebrafish, possess at least two *AHR* genes, whereas mammals seem to have only one. The two distinct classes of fish *AHR* genes have been denoted as *AHR1* and *-2* (Hahn et al., 1997). Phylogenetic comparisons suggest that a gene duplication event during early vertebrate evolution resulted in the two forms of the *AHR* (Hahn et al., 1997). The nomenclature of fish *AHRs* and *ARNTs* follows the evolutionary conventions recently reported (Hahn et al., 1997). Sequence analysis reveals that AHR1 in fish shares the greatest sequence similarity with the mammalian AHR. AHR1 and an AHR2 have been cloned in *Fundulus heteroclitus* (FhAHR1 and FhAHR2) (Karchner et al., 1999). Full-length AHR2s have been described in zebrafish (zfAHR2) (Tanguay et al., 1999), the Atlantic tomcod (Roy and Wirgin, 1997), and rainbow trout (rtAHR2α and rtAHR2β) (Abnet et al., 1999a). Full-length cDNAs for zebrafish AHR2 (*zfAHR2*) and ARNT2 (*zfARNT2*) have been cloned, and their translation products have been characterized (Tanguay et al., 1999, 2000). zfAHR2 and zfARNT2b form a functional heterodimer in vitro. The zfAHR2/zfARNT2b heterodimer specifically recognizes DREs in gel-shift experiments and induces DRE-driven transcription in response to TCDD exposure in COS-7 cells (Tanguay et al., 1999, 2000). Here, we report the cloning and characterization of a full-length zfAHR1 cDNA that corresponds to a partial fragment described previously (Wang et al., 1998). The temporal and tissue-specific expression of zfAHR1 and zfAHR2 mRNAs was compared, as were the functional properties of the two proteins. The mRNA expression patterns and functional properties of zfAHR1 and zfAHR2 proteins were found to be distinct. Finally, chimeric AHRs were constructed to delineate the domains responsible for the differential zfAHR1 and zfAHR2 activity.

Materials and Methods

Reagents, Chemicals, and Cell Culture. TCDD (>99% pure) was purchased from Chemsyn (Lenexa, KS); 2,3,7,8-tetrabromodibenzo-*p*-dioxin (TBDD; >99% pure), 3,3′,4,4′,5-pentachlorobiphenyl (PCB126; >97% pure), and 1,2,3,7,8-pentachlorodibenzo-*p*-dioxin (>99% pure) were obtained from UltraScientific (North Kingstown, RI); and 2,3,7,8-tetrachlorodibenzofuran (TCDF; >99% pure) and 2,3,4,7,8-pentachlorodibenzofuran (PeCDF; >99% pure) were provided by Dr. Linda Birnbaum (United States Environmental Protection Agency, Research Triangle Park, NC). The benzo[*a*]pyrene (BaP), indole-3-carbinol (I3C; 99% pure), 3-methylcholanthrene (3MC; 98% pure), and indole-3-acetic acid (I3AA; 98% pure) were purchased from Aldrich Chemical Co. (Milwaukee, WI) and 7,12-dimethylbenz[*a*]anthracene (DMBA) from Sigma (St. Louis, MO). β-Naphthoflavone (BNF; >99% pure) was purchased from Acros Organics (Fairlawn, NJ), and 1,2,3,4,7,8-hexachlorodibenzo-*p*-dioxin (98% pure) was obtained from Cambridge Isotope Laboratories (Woburn, MA). The chicken egg yolk phosphatidylcholine (PC; >99% pure) in chloroform was purchased from Avanti Polar Lipids (Birmingham, AL). Monkey kidney epithelial cells (COS-7) from American Type Culture Collection (Manassas, VA) were raised at 37°C in Dulbecco's modified Eagle's medium supplemented with 10% fetal calf serum in an atmosphere of 5% CO with 100% humidity.

Oligonucleotides. All oligonucleotide primers were synthesized by the University of Wisconsin Biotech Center or Invitrogen (Carlsbad, CA); they appear in Table 1. Oligonucleotides for DNA gel-shift experiments were described previously (Tanguay et al., 1999). Site-directed mutagenesis oligonucleotides are shown in Table 2.

zfAHR1 cDNA Identification and Cloning. A 552-base pair sequence in GenBank (accession number Y08433) was found to be 65% identical with the human AHR at the amino acid level (Wang et al., 1998). A PCR-based approach was used to amplify the 5′ and 3′ ends of this putative zebrafish *AHR1* sequence using the 5′-3′ rapid amplification of cDNA ends (marathon RACE) kit essentially as detailed by the manufacturer (BD Clontech, Palo Alto, CA). In brief, 2 μg of whole adult poly(A^+) RNA was reverse transcribed using avian myeloblastosis virus reverse transcriptase and the Marathon cDNA synthesis primer followed by second-strand synthesis. After universal adaptor primer ligation, 5 μl of a 1:200 dilution of the adapted cDNA was used as a template for 5′- and 3′-RACE using *zfAHR1*-specific primers F1 and R1 with the supplied adapter-specific primer using the following conditions: 30 s at 94°C and 4 min at 72°C. Five-microliter aliquots, diluted 1:200 from the original PCR reactions, were reamplified under the same conditions as above using nested F2, R2, and adaptor primers. Amplified products were visualized by ethidium bromide staining and subcloned into pGEM-T EASY (Promega, Madison, WI). Several independent clones were

TABLE 1

Primers for *AHR1* cloning

F indicates forward primers corresponding to sense strands and R indicates antisense reverse primers. Initiation ATG codons are underlined and the sequence encoding restriction sites and non–gene-encoding sequences are lowercase.

F1	5′-ATGTCATTCATCAGAGTGTGTATG-3′
F2	5′-GAAGACCGGCATGAGTTTCAG-3′
R1	5′-TTGATATCCTGAACCACTATTACAG-3′
R2	5′-CAGTTTATACTTGGTTTTGAACATTAAG-3′
F3	5′-AACTAGTCAAGGCTAAGGGTG-3′
F4	5′-gatcctgcagcCACCATGAGCTCCAGTAATATTTATG-3′
R3	5′-CGTCAAAATTTTGTCCCTTTTATC-3′
R4	5′-gatcgaattctCATATGAAGAGTTTGTTTC-3′
F5	5′-gatcctgcagccATGCTAGCACTGAAAAAAACACTC-3′

sequenced and found to contain the putative *zfAHR1* sequence. To specifically subclone the *zfAHR1* open reading frame, poly(A$^+$) RNA isolated from whole adult zebrafish RNA (200 ng) was used as a template for reverse transcriptase-PCR with the high-fidelity *Pfu* polymerase (Promega). Gene-specific primers corresponding to sequences within the 5′- (primers F3 and F4, containing *Pst*I sites) and 3′- (primer R3, with an added Eco R1 site) untranslated regions were designed to allow amplification of two distinct full-length *AHR1* cDNAs using high-fidelity *Pfu/Taq* polymerase (Promega). The initiation ATG of the F3/R3 and PCR product (*zfAHR1-*) aligned with the mammalian *AHR* initiation codon, and the F4/R3 product (*zfAHR1*) has another in-frame ATG 18 amino acids upstream.

cDNA Constructs for Functional Studies. To generate eukaryotic expression vectors pBKCMV-*zfAHR1* and pBKCMV-*zfAHR1*−, the amplicons were digested with *Pst*I and *Eco*RI and cloned into pBKCMV previously digested with *Pst*I and *Eco*RI. To generate a C-terminal FLAG-tagged zfAHR1 protein for functional studies, the pBKCMV-*zfAHR1* plasmid DNA was used as a template for PCR with the forward gene-specific primer 342 base pairs upstream of the stop site with a reverse primer encoding the FLAG epitope, the stop codon, and an *Eco*RI site (R4). The *pfu* polymerase-amplified product was cut with *Xho*I (internal site) and *Eco*RI and placed into pBKCMV-*zfAHR1* previously digested with *Xho*I and *Eco*RI to produce pBKCMV-*zfAHR1*FLAG. Restriction analysis and DNA sequencing verified all clones. Dr. Michael Denison (University of California at Davis) generously provided the dioxin-responsive luciferase reporter containing a fragment of the mouse *cyp1a1* enhancer (*pGudluc1.1*) (Garrison et al., 1996). The rainbow trout dioxin-responsive reporter (*prt1Aluc*) and the *zfAHR2* and *zfARNT2b* expression vectors (pBKCMV-*zfAHR2* and pBKCMV-*zfARNT2b*) were described previously (Tanguay et al., 1999, 2000).

Nucleotide and Amino Acid Sequence Analysis. Both strands of each clone were sequenced at least three times using fluorescent dye-labeling cycle sequencing by the Applied Biosystems-University of Florida Biotechnology Center (Gainesville, FL) stepwise using gene-specific primers before GenBank submission. Genetics Computer Group software and the Baylor College of Medicine Human Genome Center search launcher (http://searchlauncher.bcm.tmc.edu/) and the National Center for Biotechnology Information (http://www.ncbi.nlm-.nih.gov) were used for sequence analysis.

Phylogenetic Analyses. AHR amino acid sequences were aligned using ClustalX version 1.64b (Thompson et al., 1997) and were used to construct phylogenetic trees using distance (neighbor-joining algorithm) and maximal parsimony criteria (PAUP*4.0b8) (Swofford, 1998). Trees were constructed using sequences corresponding to the N-terminal 497 amino acids of the zebrafish AHR1; regions of poor or uncertain alignment were omitted. The low sequence identity among AHRs within the C-terminal halves of the proteins precludes accurate alignments, and thus, use of this region for tree construction was contraindicated. The sequences of *D. melanogaster* and *Caenorhabditis elegans* AHR homologs were used as outgroups.

TABLE 2

Site-directed mutagenesis oligonucleotides

F indicates forward primers corresponding to sense strands and R indicates antisense reverse primers. Point base substitutions are in bold.

Create *Sal*I site on the N-terminal side of the ligand-binding domains at amino acid position 240 of zfAHR1 and zfAHR2	
F6	5′-CTTCCAGGGC**GAC**TGAAGTTCTTGTATGGG-3′
R6	5′-CCCATACAAGAACTTCA**GTC**G**A**CCCTGGAAG-3′
F7	5′-CTGAACTTCCAGGG**TCGA**CTGAAATATCTC-3′
R7	5′-GGAGATATTTCAGC**GA**CCCTGGAAGTTCAG-3′
Create *Pst*I site immediately C-terminal to ligand-binding domains (amino acid position 410) of both receptors	
F8	5′-CTGAGAAACCGTGCA**C**TG**CA**GCTTCCCTTCAG-3′
R8	5′-CTGAAGGGAAGC**TG**CA**G**TGCACGGTTTCTCAG-3′
F9	5′-CTCCGTCAAAGGAAG**C**TGCA**G** CTACCATTTAACTGC-3′
R9	5′-GCAGTTAAATGGTAG**C**TGCA**G**CTTCCTTTGACGGAG-3′
Real-time PCR primers	
zfAHR1F	5′-TAGACAGCGATATACAGCAG-3′
zfAHR1R	5′-TCTCTCCAACACCATTCATG-3′
zfAHR2R	5′-AGTAGGTTTCTCTGGCCAC-3′
zfAHR2F	5′-ACGGTGAAGCTCTCCCATA-3′
zfARNT2aR	5′-CACAGTGAAATATTCCTTGATC-3′
zfARNT2F	5′-GACTGAATTCCTTTCGCGCCAC-3′
zfARNT2b/cR	5′-CTGGAGCTGCTTGACGTTG-3′
zfCYPF2	5′-TGCCGATTTCATCCCTTTCC-3′
zfCYPR2	5′-AGAGCCGTGCTGATAGTGTC-3′
β-actinF	5′-AAGCAGGAGTACGATGAGTC-3′
β-actinR	5′-TGGAGTCCTCAGATGCATTG-3′

zfAHR Chimeric Expression Constructs. Six *zfAHR1*/*zfAHR2*-FLAG chimeric constructs were produced using the QuikChange site-directed mutagenesis kit (Stratagene, La Jolla, CA) following the manufacturer's instructions. Restriction sites were engineered into *zfAHR1* and *zfAHR2* flanking each ligand-binding domain. Primers F6/R6 and F7/R7 created *Sal*I sites at amino acid positions 240 in zfAHR1 and zfAHR2, respectively. Primers F8/R8 and F9/R9 created *Pst*I sites at amino acid positions 410 in zfAHR1 and zfAHR2, respectively. The ligand-binding domains of *zfAHR1* and *zfAHR2* were swapped by cutting each construct with *Sal*I and *Pst*I, followed by gel isolation and ligation to create *zfAHR1* with the ligand-binding domain of *zfAHR2* (*zfAHR1-2LBD*) and *zfAHR2* with the ligand-binding domain of *zfAHR1* (*zfAHR2-1LBD*). Additional chimera constructs were designed to swap the bHLH-PAS, LBD, or C-terminal domains, so each protein can be designated to contain three segments. To create constructs containing the bHLH and PAS domains from *zfAHR1* fused to the ligand-binding and C-terminal transactivation domains of *zfAHR2* and the bHLH and PAS domains from *zfAHR2* fused to the ligand-binding and C-terminal transactivation domains of *zfAHR1*, each construct was cut with *Sal*I and *Not*I (polylinker site) followed by gel isolation and ligation to create chimeric constructs 1-2-2 and 2-1-1, respectively. To create fusion constructs containing the bHLH, PAS, and ligand-binding domain from *zfAHR1* fused to the C-terminal transactivation domain of *zfAHR2* and the bHLH PAS and ligand-binding domain from *zfAHR2* fused to the C-terminal transactivation domain of *zfAHR1*, each construct was cut with *Pst*I and *Not*I followed by gel isolation and ligation to create chimeric constructs 1-1-2 and 2-2-1, respectively (diagrammed in Fig. 11B). Restriction digestion, DNA sequencing, and in vitro translation confirmed the proper construction of each clone.

Gene Mapping. The LN54 RH panel (a hybrid between zebrafish and mouse cells) was obtained from Dr. Marc Ekker (Loeb Health Research Institute, Ottawa, ON, Canada). This panel of 94 DNAs was used to map the chromosomal location of *zfAHR1* and *zfAHR2* according to methods described previously (Hukriede et al., 1999). In brief, PCR reactions containing 100 ng of hybrid-cell DNA from each of the parental cell lines, 0.25 μM of each oligonucleotide primer, 10 mM Tris-HCl, pH 8.3, 50 mM KCl, 1.5 mM $MgCl_2$, 0.2 mM each of dATP, dCTP, dGTP, and dTTP, and 1 unit of *Taq* DNA polymerase were used, in a total volume of 20 μl. PCR was performed for 32 cycles: 30 s at 94°C, 30 s at the appropriate annealing temperature for a given primer set, and 30 s at 72°C. PCR products were separated on 1.5% agarose and visualized by ethidium bromide staining. All PCR assays were performed in duplicate before linkage group assignment.

Embryonic TCDD Exposure, Poly(A$^+$) RNA Isolation, and Northern Analysis. Five hundred zebrafish embryos within 3 h of fertilization were exposed to 40 ml of 0.2% acetone or TCDD dissolved in 1.55 μM acetone for 1 h. After exposure, embryos were washed with TCDD-free water and allowed to develop in 150-mm culture plates at 27°C. Culture media was exchanged twice daily. At 120 h postfertilization (hpf), fish were anesthetized with tricaine methanesulfonate (MS-222), euthanized, frozen in liquid nitrogen, and pulverized, and poly(A$^+$)RNA was extracted using the PolyATract system (Promega). Five micrograms of mRNA was electrophoresed on a 1.2% agarose formaldehyde gel and transferred to Hybond+ membrane (Amersham Biosciences, Piscataway, NJ). The membrane was prehybridized and hybridized in 6× standard saline

citrate, 0.1% SDS, and 50% formaldehyde at 42°C with random primed [^{32}P]cDNA probes. The blot was sequentially probed with random primed zfAHR1, zfAHR2, zfCYP1A, and β-actin-specific probes. Exposure times for the probes were zfAHR1, 4 days; zfAHR2, 2 days; zfCYP1A, 1 day; and β-actin, 12 h. Intensity of each band was determined by phosphorimaging (PhosphorImager; Molecular Dynamics, Sunnyvale, CA). The intensity of each band was normalized to β-actin expression.

Adult TCDD Exposure. Liposomes incorporated with or without TCDD were prepared with chicken egg yolk PC. In brief, TCDD in anhydrous 1,4-dioxane was dried in a glass vial under nitrogen and reconstituted in chloroform. PC at 10 μM was added to the TCDD-chloroform mixture and dried under vacuum using a rotary evaporator. The PC and TCDD mixture was reconstituted in saline (0.9%), resulting in a final concentration of 50 μM PC. Liposomes were formed by first vortexing and then sonicating the reconstituted PC and TCDD mixture. Adult male zebrafish were injected i.p. with either PC or PC containing TCDD at a final dose of 10 ng of TCDD/g of fish.

Developmental Expression of zfAHR1 and Quantitative Tissue-Specific Distribution of zfAHR1, zfAHR2, and zfCYP1A mRNAs. To quantify zfAHR1 mRNA abundance during development, 25 groups of 50 embryos per group were exposed to either vehicle or TCDD as above for real-time quantitative reverse transcriptase-PCR. Embryos were euthanized at 24, 36, 48, 72, and 120 hpf, respectively (five groups/treatment at each time), frozen in liquid nitrogen, and stored at −70°C for RNA isolation. Total RNA was isolated from each vehicle control and TCDD-treated group. mRNA expression also was determined in adult zebrafish by dissecting tissues from 6-month-old adult male zebrafish injected i.p. with PC vehicle or PC containing TCDD as described above. Fish were maintained for 3 days before euthanasia and collection of various organs. The organs from six groups of vehicle-exposed and TCDD-exposed fish, respectively (n = 5 fish/group), were used for RNA isolation. Tissues were shredded using glass beads according to the manufacturer (QIAGEN, Valencia, CA), and RNA was isolated using Qiashredder homogenizers (QIAGEN) and TRI reagent (Molecular Research Laboratories, Cincinnati, OH) according to the manufacturer's instructions from the brain, eye, fins (caudal, pectoral, pelvic, and dorsal), gills, heart, kidney, liver, skeletal muscle, skin, and swimbladder. One microgram of total RNA from each group of fish was resolved on a 1% denaturing formaldehyde agarose gel to ensure the quality and concentration of the RNA. cDNA was produced from 2 μg of each RNA pool using Superscript II (Invitrogen) and the oligo(dT) primer in a 20-μl volume. The Light Cycler (Roche Applied Science, Indianapolis, IN) was used for quantitative real-time PCR. One microliter of each cDNA pool was used for each PCR reaction in the presence of SYBR Green according to the manufacturer's instructions. Agarose gel electrophoresis and thermal denaturation (melt curve analysis) were used to confirm specific product formation.

Velocity Sedimentation Analysis. 2,3,7,8-Tetrachloro[1,6-^{3}H]dibenzo-p-dioxin ([^{3}H]TCDD; 34.7 Ci/mmol) and [3′,5′-^{3}H]β-naphthoflavone ([^{3}H]BNF; 18.75 Ci/mmol; ≥98% radiochemical purity) were obtained from Chemsyn (Lenexa, KS). The [^{3}H]TCDD was purified to ≅95% by high-performance liquid chromatography as described previously (Gasiewicz and Neal, 1979). TCDF was obtained from UltraScientific. Methylated-[*methyl*-^{14}C]-ovalbumin was from PerkinElmer Life Sciences (Boston, MA). Methylated-[*methyl*-^{14}C]catalase was synthesized as described previously (Dottavio-Martin and Ravel, 1978). zfAHR1, zfAHR2, and human AHR proteins were expressed by in vitro transcription and translation (TNT) and analyzed by velocity sedimentation on sucrose gradients in a vertical tube rotor. For each AHR, two identical TNT reactions (100 μl total) were combined, diluted 1:1 with MEEDMG buffer [25 mM MOPS, pH 7.5, 20°C, containing 1 mM dithiothreitol, 1 mM EDTA, 5 mM EGTA, 0.02% NaN_3, 20 mM Na_2MoO_4, and 10% (v/v) glycerol], split into two 100-μl aliquots, and incubated with [^{3}H]TCDD ± unlabeled TCDF (100-fold excess) or [^{3}H]BNF ± unlabeled BNF (100-fold excess) for 2 h or overnight (18 h) at 4°C. [^{3}H]TCDD or [^{3}H]BNF concentrations were verified by sampling each tube for total counts. No charcoal-dextran treatment was used to remove unbound [^{3}H]TCDD, because fish AHRs have been shown to be sensitive to small amounts of charcoal (Lorenzen and Okey, 1990). After incubation, 95 μl of each incubation was applied to 10 to 30% sucrose gradients, and the tubes were spun for 140 min at 60,000 rpm at 4°C in a VTi 65.2 rotor. Gradients were fractionated (150 μl per fraction) and counted using a LS5000TD scintillation counter (Beckman Coulter, Inc., Fullerton, CA). Specific binding is defined as the difference between total binding (incubations containing radioligand) and nonspecific binding [incubations containing radioligand plus a 100-fold excess of unlabeled ligand or incubations of radioligand with TNT reactions containing an empty vector (referred to as "unprogrammed lysate")]. [^{14}C]catalase (11.3 S) and [^{14}C]ovalbumin (3.6 S) were added as internal sedimentation markers; they eluted in fractions indicated in the figure legends. In one experiment, zfAHRs and zfARNT2 were coexpressed in the presence of [^{3}H]TCDD (as described below for DNA binding assays, except in the presence of 5 nM [^{3}H]TCDD) before fractionation by velocity sedimentation. See figure legends for details.

In Vitro Expression of zfAHR Proteins and In Vitro DNA Binding Assay. For in vitro DNA binding assays, recombinant zebrafish proteins were produced from the pBK-CMV expression constructs with T3 RNA polymerase using the TNT-coupled rabbit reticulocyte lysate as described by the manufacturer (Promega). We have found that coexpressing the AHR and ARNT proteins in the TNT reaction in the presence of 10 nM TCDD before gel-shift analysis significantly increased the amount of the AHR/ARNT/DRE complex. Side reactions containing [^{35}S]methionine were performed to assess relative protein production. After the 90 min incubation at 30°C, radioactive translation products were resolved by 8% SDS polyacrylamide gel electrophoresis (SDS-PAGE), dried, and phosphorimaged. Unlabeled reactions were stored at −70°C before functional studies. In vitro gel-shift analysis was performed as described previously (Tanguay et al., 1999). Approximately four times as much zfAHR1 or zfAHR2 was coexpressed with zfARNT2b and incubated in the presence of 10 nM TCDD in 0.2% DMSO or DMSO alone for 20 min at 22°C. After incubation, 1.5 μg of poly(dI-dC) and binding buffer [20 mM HEPES, pH 7.9, 100 mM NaCl, 1 mM dithiothreitol (DTT), and 6% glycerol] was added and the incubation continued for an additional 20 min at 22°C. In some reactions, 1 μg of affinity-purified monoclonal mouse anti-ARNT2 (M-20, Santa Cruz Biotechnology, Inc., Santa Cruz, CA) or mouse anti-zebrafish collagen (Institute of Neuroscience, University of Oregon, Eugene, OR) antibodies were added before the addition of 50,000 cpm of the rtDRE and 10-fold molar excess of unlabeled wild-type rtDRE or mutated rtDRE competitor DNAs. After 20 min of incubation at 22°C, complexes were resolved on a 0.5× Tris/borate/EDTA (90 mM Tris, 64.6 mM boric acid, and 2.5 mM EDTA, pH 8.3) and 4.5% acrylamide gel at 22°C. The dried gels were exposed to a phosphor screen for 2 days before analysis.

Production of Total COS-7 Cell Lysate and Detection of FLAG-Tagged zfAHRs. COS-7 cells at 70% confluence in 60-mm Petri dishes were transfected with 5 μg of pBK-CMV-*zfAHR1*FLAG, pBK-CMV-*zfAHR2*FLAG, or empty pBK-CMV DNA using SuperFect (QIAGEN) as detailed by the manufacturer. Whole-cell lysate was harvested 20 h later essentially as described previously (Hahn et al., 1994). In brief, the cells were rinsed twice with phosphate-buffered saline (137 mM NaCl, 2.7 mM KCl, 8 mM Na_2PO_4, and 1.5 mM KH_2P0_4, pH 7.4) containing EDTA and EGTA (1 mM each), removed from the dish using a Teflon spatula, rinsed with 300 μl of extraction buffer [25 mM MOPS, pH 7.5, containing 1 mM EDTA, 5 mM EGTA, 0.02% NaN_3, 20 mM Na_2MoO_4, 10% (v/v) glycerol, 1 mM DTT, 5 μg/ml leupeptin, 1 μg/ml aprotinin, and 5 μg/ml pepstatin A], and transferred into a 1.5-ml centrifuge tube on ice. Cells were sonicated three times on ice and homogenized using a Dounce homogenizer. Debris was pelleted by centrifugation at 22,000g for 30 min, and the

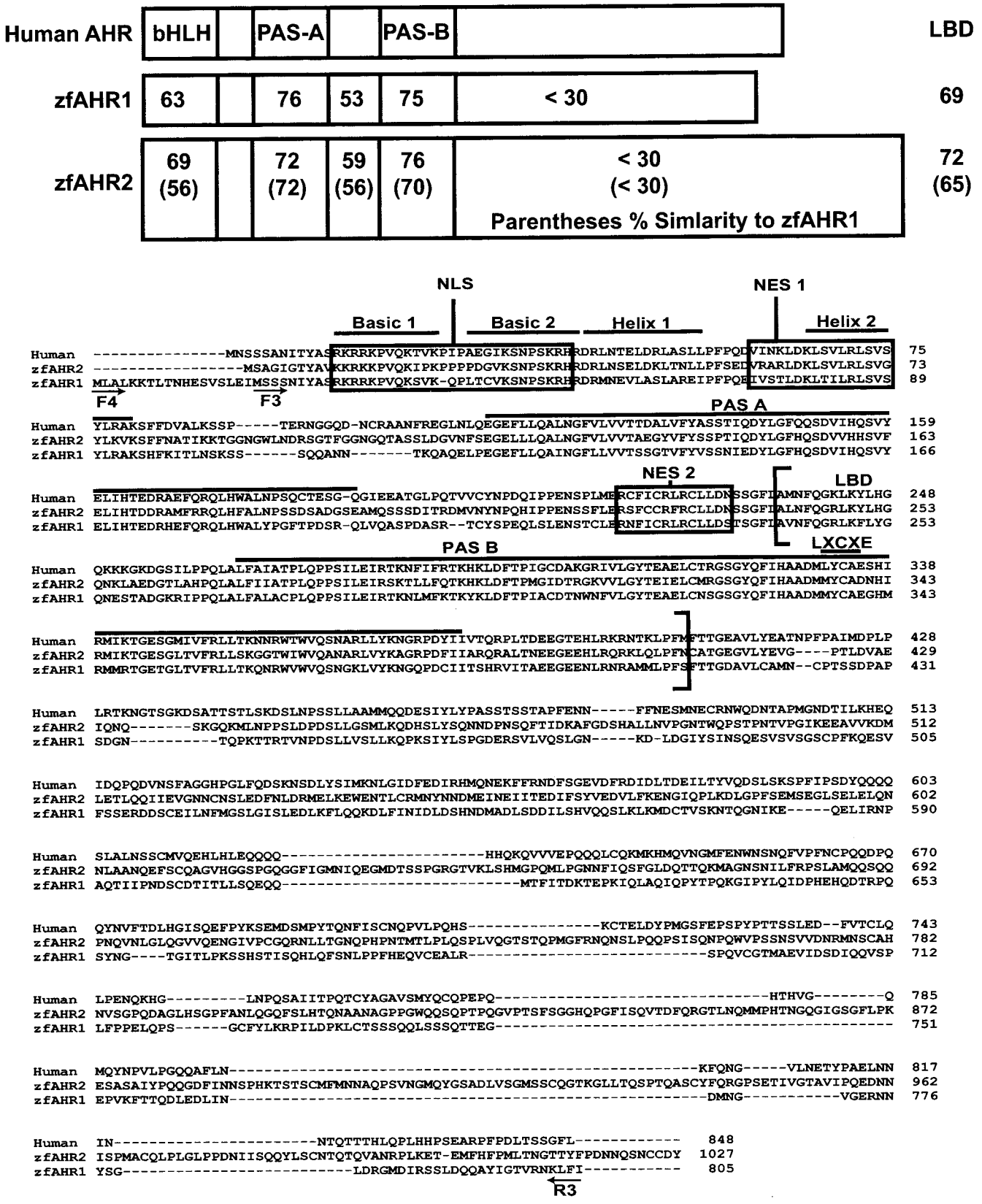

Fig. 1. Amino acid sequence alignment of zfAHR1, zfAHR2, and the human AHR. Sequence alignment was done using ClustalW1.8. The percentage identity to the human AHR within each region is indicated at the top of the figure. The numbers in parentheses indicate the regional percent identity between zfAHR1 and zfAHR2. Dashes indicate gaps in sequence alignment. Functional domains: bHLH, PAS, and ligand binding (Coumailleau et al., 1995; Fukunaga et al., 1995). NLS, nuclear localization signal (Ikuta et al., 1998); NES 1, nuclear export signal 1 (Ikuta et al., 1998); NES 2, nuclear export signal 2 (Berg and Pongratz, 2001); and LXCXE, potential retinoblastoma protein binding site (Puga et al., 2000). The bracketed sequence signifies the ligand-binding domain. zfAHR1, AF258854; zfAHR2, AF063446; human AHR, L19872.

protein concentrations were determined by the Bradford protein assay using bovine serum albumin as a standard. To evaluate FLAG-tagged zfAHR protein expression, 20 μg of each COS-7 cell lysate was resolved by SDS-PAGE on an 8% gel and transferred to nitrocellulose. Immunochemical detection was carried out by blocking the blot with 5% dry milk in TBS-T [25 mM Tris, pH 7.6, 150 mM NaCl, and 0.1% Tween 20] for 1 h followed by two TBS-T washes. The FLAG epitope was then detected by incubation with 2 μg/ml anti-FLAG monoclonal antibody (Sigma) diluted in TBS-T containing 1% dry milk. The antibody was removed after 2 h and blots were washed with TBS-T three times. Horseradish peroxidase-conjugate secondary antibody (Amersham Biosciences) diluted 1:4000 in TBS-T containing 5% dry milk was added for a 1-h incubation. Blots were washed three times in TBS-T before chemiluminescence detection (Amersham Biosciences). X-ray film was digitally scanned and printed from PhotoShop 6.0 (Adobe Systems, Mountain View, CA).

Transient Transfection. COS-7 cells were plated on 24-well plates at a density of 6×10^4 cells per well 1 day before transfection. Transient transfections were conducted using SuperFect (QIAGEN). Each well was cotransfected with 400 μl of serum-containing media including wild-type or chimeric *zfAHRs* (450 ng) and *zfARNT2b* (450 ng) expression vectors, 100 ng of a luciferase reporter (*prt1Aluc* or *pGudluc1.1*), and a β-galactosidase CMV reporter (50 ng) for estimation of transfection efficiency. After a 2-h incubation at 37°C, transfection media was removed and replaced with 1 ml of fresh serum-containing media to each well. After a 20-h incubation, cells were exposed to DMSO vehicle (control), TCDD, or the indicated ligand previously dissolved in DMSO (0.1% media volume). Cells were harvested after 20 h of incubation. Media were aspirated, and each well washed with 0.5 ml of phosphate-buffered saline. One hundred microliters of lysis buffer was added to each well (100 mM KPO_4, pH 7.8, 6 mM $MgSO_4$, 0.1% Triton X-100, 1 mM DTT, and 4 mM ATP trihydrate). A 10-μl aliquot of cell lysate was transferred to a 96-well luminometer and 50 μl of luciferase assay buffer (Promega) was injected into each well and incubated for 2 s, and luminescence was integrated over 10 s. Luciferase assays were completed using either a ML-2250 luminometer (Dynatech Labs, Chantilly, VA) or a Monolight 2010 luminometer (Analytical Luminescence Laboratory, Ann Arbor, MI). β-Galactosidase activity was determined for each well as follows. Fifteen microliters of cell lysate was aliquoted to a 96-well plate. Two hundred microliters of reaction buffer (0.1 M $NaPO_4$, 10 mM KCl, 1 mM $MgCl_2$, and 0.385% β-mercaptoethanol) was added to each well followed by the addition of 40 μl of 4 mg/ml *o*-nitrophenyl-β-D-galactopyranoside. The reaction was then incubated at 37°C for 2 to 4 h. Plates were read at 405 nM using an ELx800 plate reader (Bio-Tek Instruments, Winooski, VT).

Statistical Analysis. Abundance of mRNAs detected by quantitative real-time PCR was expressed as mean ± S.E.M. Significance of stage of development and TCDD exposure on *zfAHR1* mRNA abundance was tested using a two-way ANOVA on $\log_{10}$ transformed data. In brief, five groups of zebrafish embryos ($n = 50$ embryos/group) were exposed to vehicle or TCDD and analyzed for gene-specific mRNA expression. Differences among groups attributable to treatment or development stage were analyzed using the Tukey method, and differences among means were considered significant at $p < 0.05$. The significance of differences in tissue-specific expression and in the effect of TCDD exposure on mRNA abundance was tested using a one-way ANOVA on $\log_{10}$ transformed data. Differences among groups were analyzed using the Tukey method ($p < 0.05$). The effects of potential AHR ligands on zfAHR activation in transient transfection assays were assessed by one-way ANOVA. Significant differences from vehicle control and TCDD treatment groups were determined by Dunnet's analysis ($p < 0.05$). All statistical analyses were performed using SigmaStat software (Chicago, IL).

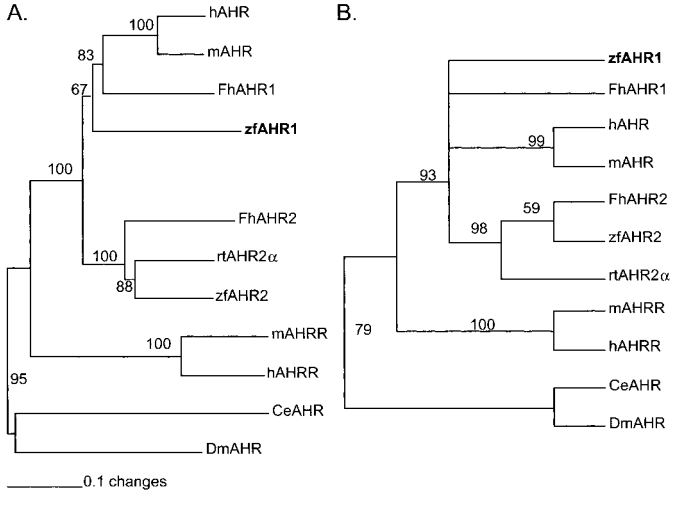

Fig. 2. Phylogenetic analysis of aryl hydrocarbon receptor amino acid sequences. AHR amino acid sequences were aligned, and the alignments were used to construct phylogenetic trees as described under *Materials and Methods*. Trees were constructed using sequences corresponding to the N-terminal 497 amino acids of the zebrafish AHR1; regions of poor or uncertain alignment were omitted. The sequences of *D. melanogaster* and *C. elegans* AHR homologs were used as outgroups. A, neighbor-joining tree. Numbers next to branch points are bootstrap values based on 100 resampling. B, majority-rule consensus tree obtained by maximal parsimony analysis, using the branch-and-bound search algorithm and a bootstrap analysis based on 100 resamplings of the alignment. The analysis included 246 informative characters. The GenBank accession numbers of the AHR sequences used are: *Homo sapiens* (Hs) AHR (L19872), *Mus musculus* (Mm) AHR (M94623), *F. heteroclitus* (Fh) AHR1 (AF024591), *F. heteroclitus* (Fh) AHR2 (U29679), zfAHR1 (AF258854), zfAHR2 (AF063446), rainbow trout rtAHR2α (AF065137), *M. musculus* AHRR (AB015140), human AHRR (AB033060), *D. melanogaster* (Dm) AHR (AF050630), and C. *elegans* (Ce) AHR (AF039570).

Results

Identification of zfAHR1 cDNA. After identification of a partial AHR-like sequence in GenBank, we used a nested PCR-based 5′- and 3′-RACE approach to identify and clone the zfAHR1 cDNA (see *Materials and Methods*). The nucleotide sequence for *zfAHR1* has been deposited in the GenBank database under accession number AF258854. There are several zfAHR1 characteristics worth noting (Fig. 1). The cDNA encodes an 805-amino acid protein with a theoretical molecular mass of 90.4 kDa. Alignment of zfAHR1 with zfAHR2 and the human AHR illustrates that the greatest similarity lies within the bHLH and PAS domains (Fig. 1). Zebrafish AHR1 and AHR2 share 40% amino acid identity overall and 58% in the N-terminal half, which contains the bHLH and PAS functional domains. Zebrafish AHR1 and the human AHR share 43% amino acid identity overall and 65% in the N-terminal half. As with all reported AHRs, the C-terminal domain sequences are divergent, and it is also apparent that zfAHR1, like zfAHR2, lacks the Q-rich domain, important for transactivation in mammalian AHRs (Fukunaga et al., 1995).

Phylogenetic analysis and gene mapping were used to determine the relationship of *zfAHR1* to other *AHR*-like genes in mammals, fish, and invertebrates. The trees shown in Fig. 2 clearly demonstrate that *zfAHR1* is a member of the vertebrate AHR clade, which includes mammalian AHRs, fish AHR1 and AHR2s, and mammalian AHR repressors. In addition, this analysis reveals that the zfAHR1 protein is most closely related to the mammalian/fish AHR(1) clade and is clearly distinct from the clade containing zfAHR2 and other fish AHR2s and from the AHR repressor clade. To further confirm that the *zfAHR1* and *zfAHR2* genes are distinct, they

were mapped by PCR using the LN54 radiation hybrid panel (a hybrid between zebrafish and mouse cells) in collaboration with Dr. Marc Ekker (Loeb Health Research Institute) (Hukriede et al., 1999). The zebrafish *AHR1* gene maps to linkage group 16 in a region that shares conserved synteny with human chromosome 7, which contains the human *AHR* (Le Beau et al., 1994; Barbazuk et al., 2000). *zfAHR2* maps to a separate linkage group (LG22), which has no known conserved synteny with human chromosome 7 (Woods et al., 2000). Taken together, these results establish that *zfAHR1* is an ortholog of the mammalian *AHR*(1)s.

Developmental Expression and Adult Tissue Distribution of zfAHR1 and zfAHR2 mRNAs. To directly detect zfAHRs and zfCYP1A mRNAs, poly(A$^+$) RNA was extracted from pooled 120-hpf zebrafish larva that were previously exposed to TCDD or to vehicle control for Northern analysis. A single 3.0-kb transcript was detected with the zfAHR1-specific probe, and the abundance of this transcript seemed to be slightly elevated by TCDD exposure (Fig. 3). The zfAHR2-specific probe detected a 7.4-kb band that was also slightly elevated in response to TCDD as previously reported (Tanguay et al., 1999). The zfCYP1A probe hybridized to a 2.6-kb band only in RNA extracted from TCDD-exposed larvae. Quantitative real-time PCR was used to measure the abundance of zfAHR1 mRNAs in zebrafish larvae exposed to TCDD or vehicle and evaluated at several subsequent developmental time points (Fig. 3B). cDNA was created from RNA isolated from zebrafish at 24, 36, 48, 72, 96, and 120 hpf.

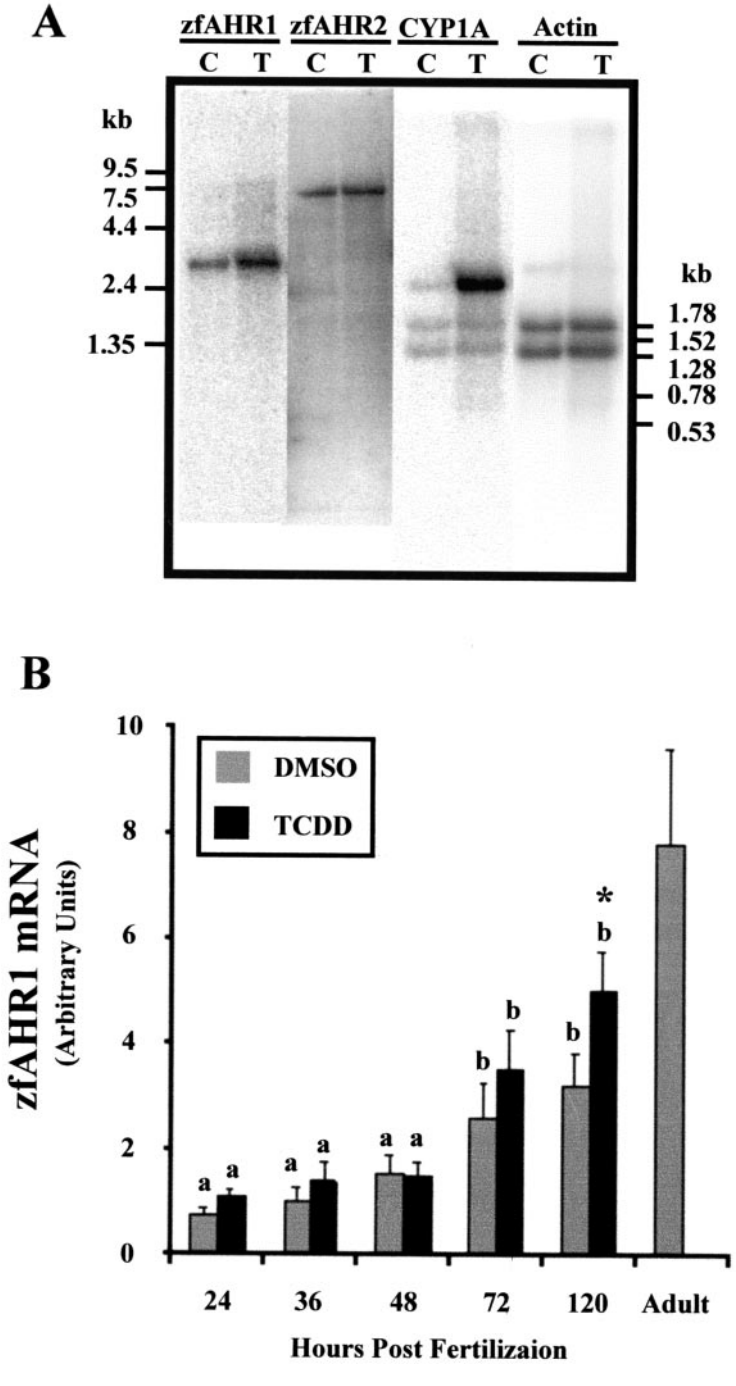

Fig. 3. Presence of zfAHR1, zfAHR2, and zfCYP1A mRNAs in zebrafish larva. A, Northern blot of poly(A$^+$) mRNA from 120-hpf whole zebrafish larva. Embryos were treated with a waterborne LC_{100} (1.55 μM) concentration of TCDD within 3 h of fertilization. Five micrograms of mRNA was resolved in each lane. Molecular mass markers, indicated on the left and right of the images in kilobases (kb) confirmed estimated size of each specific band. The blot was sequentially probed with random-primed cDNA probes for zfAHR1, zfAHR2, zfCYP1A, and rat β-actin. Abundance of message was detected by exposure to phosphor screen. Exposure times for the probes were zfAHR1 (4 days), zfAHR2 (2 days), zfCYP1A (1 day), and β-actin (12 h). B, time course of zfAHR1 mRNA expression in vehicle (control) and TCDD-exposed embryos by quantitative real-time PCR. Samples were run concurrently with standard curves derived from plasmid cDNA dilutions. zfAHR1 expression values were normalized to actin mRNA levels. The height of each bar represents the mean ± S.E.M. (n = 5). * indicates significantly different from control at the same time ($p < 0.05$). a and b indicate two groups with similar mRNA abundance.

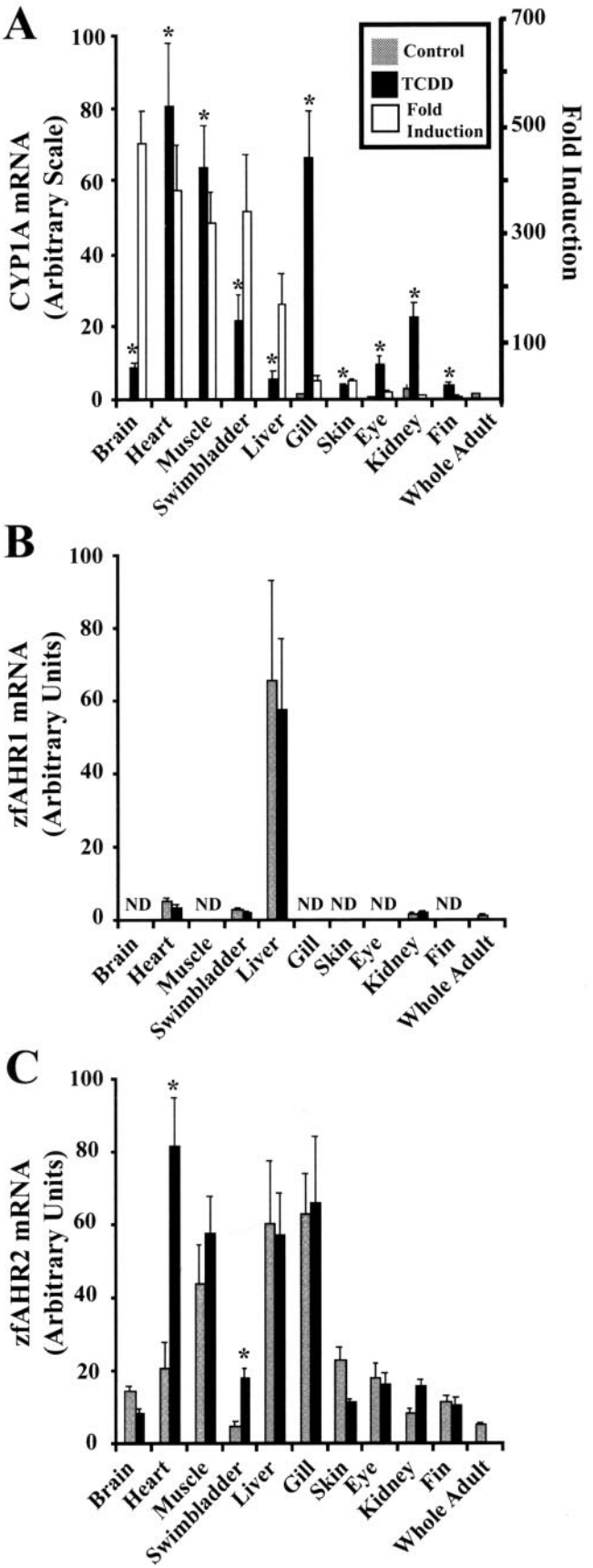

Fig. 4. Tissue distribution of zfAHR1, zfAHR2, and zfCYP1A mRNA abundance in adult male zebrafish treated with vehicle or TCDD. Gene-specific primers were used to quantify mRNAs using real-time PCR. zfCYP1A (A) tissues are organized with decreasing response (based on fold induction) to TCDD-induced zfCYP1A expression from left to right. zfAHR1 (B) and zfAHR2 (C) samples were run concurrently with standard curves derived from plasmid cDNA dilutions for each primer set. Values for each primer pair were normalized to actin mRNA levels. Each bar represents the mean ± S.E.M. ($n = 5$). One-way ANOVA was conducted to determine differences in tissue expression and was followed by Tukey's test. * indicates significant difference in the same tissue between vehicle (control) and TCDD-exposed larva ($p < 0.05$).

zfAHR1 mRNA abundance was low but detectable at 24 hpf and increased by 72 hpf with little change in expression at the later time points. Results from the quantitative real-time PCR validated the Northern analysis in that zfAHR1 was slightly elevated in larva that were exposed to TCDD. Similar results have been reported for zfAHR2 mRNA. zfAHR2 mRNA is detected at 24 hpf with elevated expression at 48, 72, and 120 hpf (Andreasen et al., 2002).

To identify the tissue-specific localization of zfAHR1, zfAHR2, zfARNT2b/c, and zfCYP1A, total RNA was isolated from organs of adult male zebrafish dosed i.p. with TCDD or vehicle, and gene expression was quantified using real-time PCR. zfCYP1A mRNA levels were used as a measure of an activated AHR signal transduction pathway. TCDD exposure resulted in significantly induced expression of CYP1A in all tissues (Fig. 4A). The rank order for the highest level of TCDD-induced CYP1A mRNA expression was the heart > gill > skeletal muscle > swimbladder > kidney > eye > liver > skin > fin. The sensitivity of this assay allows for the determination of the basal (control) CYP1A mRNA levels, therefore, TCDD-induced fold induction can be calculated for each tissue. Based on fold-induction values, zfCYP1A mRNA was most highly induced in the brain, heart, skeletal muscle, swimbladder, and liver and to a lesser, but still significant, level in the gills, skin, eye, kidney, and fins (Fig. 4A). To determine the role of individual zfAHRs in the observed CYP1A mRNA induction, the same cDNA samples were used to quantify zfAHR1 and zfAHR2 in each tissue. zfAHR1 mRNA was not widely expressed, because it was detected primarily in the liver and marginally in the heart and kidney (Fig. 4B). Moreover, TCDD exposure had no effect on the abundance or organ distribution of zfAHR1 message (Fig. 4B). The developmental expression pattern of zfAHR1 mRNA in whole embryos supports its localization primarily in the liver, because the liver is of negligible size until 72 hpf and it grows thereafter. zfAHR2, on the other hand, was expressed in all tissues examined with the highest expression in the skeletal muscle, liver, and gills (Fig. 4C). Lower levels of zfAHR2 mRNA were also measured in the brain, heart, swimbladder, skin, eye, kidney, and fins. TCDD exposure also led to a small, but significant, elevation in zfAHR2 mRNA in the heart (4-fold) and swimbladder (3.5-fold).

Differential Binding Ability of zfAHR1 and zfAHR2 to the Dioxin Response Element. As a first step in comparing the functional properties of zfAHR1 and zfAHR2, the proteins were produced in vitro using rabbit reticulocyte lysate (Fig. 5A). The zfAHR1 protein has an apparent molecular mass of 97.5 kDa and zfAHR2 and zfARNT2 have been described previously as having apparent molecular masses of 123 and 90 kDa, respectively (Tanguay et al., 1999, 2000). We and others have found that the in vitro DNA protein interactions among fish AHR, ARNT, and the DRE are weak compared with similar experiments using mammalian pro-

teins (Pollenz and Necela, 2000); however, we have observed that specific interaction between zfAHRs, zfARNT2b, and DREs can be enhanced by coexpressing the proteins in rabbit reticulocyte lysate. zfAHRs and zfARNT2b were coexpressed (Fig. 5A, lanes 4–7,) in the presence or absence of TCDD for use in DNA gel-shift experiments. For these experiments, we tested the ability of zfARNT2b to interact with zfAHR1 and zfAHR2 and bind to a radiolabeled probe containing DREs derived from the rainbow trout *cyp1a1* gene as described previously (Tanguay et al., 2000). As was previously reported, the specific complexes migrate as doublets, both of which are enhanced by ligand exposure. This doublet could arise from interactions with other proteins in the lysate or, perhaps, from uncontrolled partial protein degradation; however, we have used several protease inhibitors with no affect on the observed gel-shift activity (data not shown). In addition, the specific doublet could arise from alternate conformational configurations of the zebrafish proteins because the complexes were separated under nondenaturing conditions. Importantly, the presence of the two specific complexes is zebrafish ARNT2 specific, because zfAHR2 and the rainbow trout ARNTb only form a single specific complex (Tanguay et al., 1999). The binding observed with either zfAHR1 or zfAHR2 was specific, because the complexes were effectively competed by a 10-fold molar excess of unlabeled rtDRE (Fig. 5B, lanes 4 and 12), whereas rtDREs with a single base change in the core sequence failed to compete (Fig. 5B, lanes 5 and 13). We observed no specific complexes when zfAHR1, zfAHR2, or zfARNT2b was added separately; however, there are two lysate-derived nonspecific bands in all lanes. To further demonstrate specificity, the complexes were supershifted using the monoclonal anti-ARNT2 antibody (Fig. 5B, lanes 6 and 14). Both of the specific complexes contain zfARNT2 because both complexes are supershifted using the ARNT2 antibody. A control antibody specific for zebrafish collagen did not affect the complexes (lanes 7 and 15). These results clearly demonstrate that zfAHR1 and zfAHR2 are able to dimerize with zfARNT2b and recognize DREs in vitro. However, it is important to note that zfAHR1 gel-shift activity is significantly weaker than zfAHR2 activity. This differential DNA binding activity cannot be explained by reduced expression, because each reaction contained similar levels of AHR, but rather suggest structural and functional differences between zfAHR1 and zfAHR2.

Transactivation Activity of zfAHR1 and zfAHR2 in COS-7 Cells. To determine whether the reduced zfAHR1 gel-shift activity would result in similarly weak *trans*-activation activity, we compared the ability of zfAHR1 and zfAHR2 to activate a DRE-driven luciferase reporter upon exposure to TCDD. COS-7 cells were transiently transfected with expression constructs for either zfAHR1 or zfAHR2 along with zfARNT2b and a DRE-driven luciferase construct *pGud-luc1.1* (Garrison et al., 1996) as described previously (Tanguay et al., 1999). Cells transfected with zfAHR2 show measurable constitutive luciferase activity, which is significantly enhanced by 10 nM TCDD exposure. Cells expressing zfAHR1 possess very low constitutive and TCDD-induced luciferase activity (Fig. 6). One possible explanation for the lack of zfAHR1 transactivation activity in COS-7 cells is that the zfAHR1 is not efficiently expressed in COS-7 cells. To explore this possibility, COS-7 cells were transfected with FLAG-tagged (Sigma) *zfAHR1* or *zfAHR2* followed by total

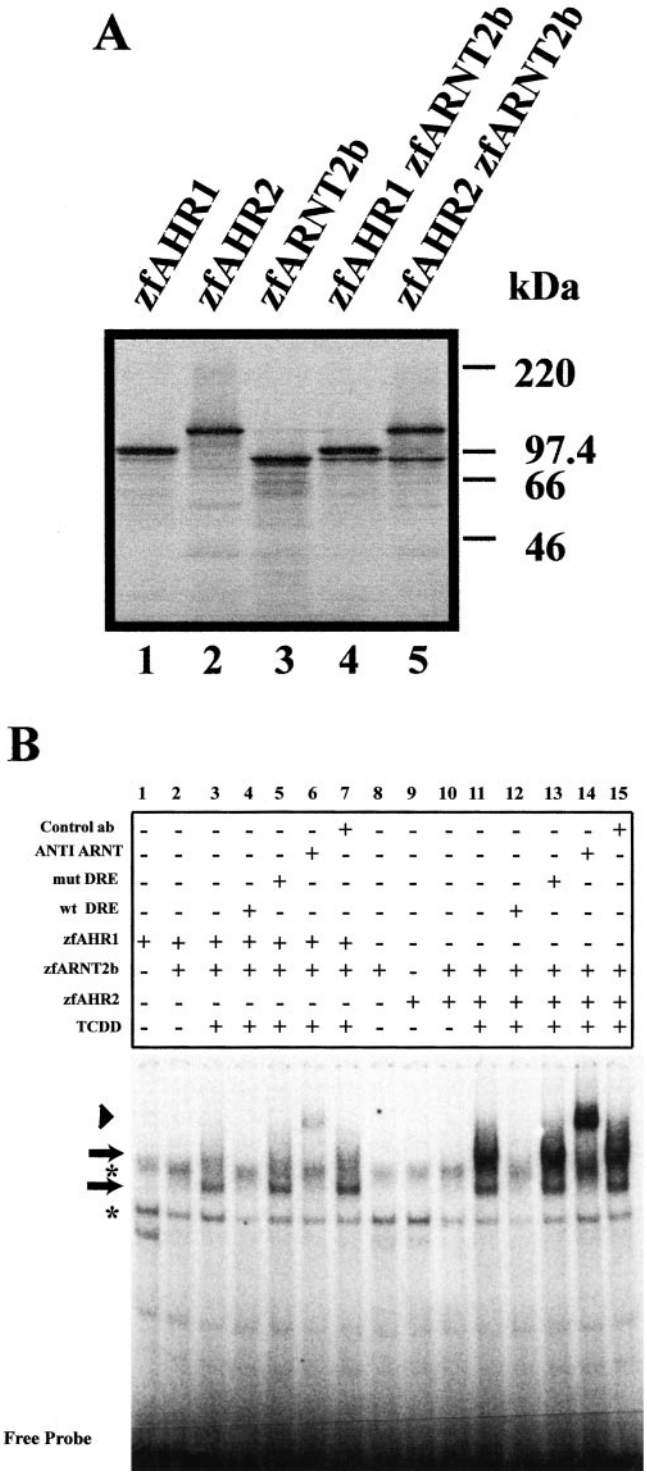

Fig. 5. Gel-shift analysis determining the specificity of interaction between zfAHR(s), zfARNT2b, and a dioxin response element (DRE). A, proteins used in gel-shift analysis were transcribed in vitro. A subfraction was expressed in the presence of [^{35}S]methionine and resolved on an 8% SDS-PAGE gel. A 4-fold zfAHR plasmid molar excess was used compared with FLAGzfARNT2b in each reaction. Phosphor image of the dried gel is shown. zfAHR1, zfAHR2, and FlagzfARNT2b were transcribed and translated alone (lanes 1–3) or in combination (lane 4–5) in the absence or presence of 10 nM TCDD. B, in vitro-translated proteins were incubated in the presence of 10-fold-molar excess wild-type or mutant DRE ^{32}P-labeled probes. The two arrows indicate specific interactions among zfAHRs, FLAGzfARNT2b, and the DRE. The arrowhead indicates the presence of a supershifted complex with the anti-ARNT2-specific antibody. The asterisks indicate nonspecific bands.

lysate production and immunoblot detection with anti-FLAG antibody. Although the FLAG antibody detects several other bands in the total lysate (Fig. 7, asterisk), it is apparent that zfAHR1 and zfAHR2 are expressed at similar levels (Fig. 7, arrows), ruling out differential expression as the primary reason for differential responsiveness in the transactivation assay. Finally, to test the hypothesis that zfAHR1 prefers to function with other zebrafish ARNT proteins, we found that zfAHR1 fails to induce reporter gene activity when transiently transfected with the known splice variants of zebrafish ARNT2 (data not shown).

Radioligand Binding Assays. The weak gel-shift activity and the lack of TCDD-induced transcriptional activity suggested that the zfAHR1 may be deficient in its ability to bind TCDD. To investigate this possibility, the specific binding of [^{3}H]TCDD to in vitro-translated zfAHR1 and zfAHR2 proteins was assessed by velocity sedimentation on sucrose gradients. When assayed under a variety of conditions (2–10 nM [^{3}H]TCDD; 2- to 18-h incubation time; and low and high salt) in several experiments, the human AHR and zfAHR2 exhibited substantial peaks of [^{3}H]TCDD-specific binding (i.e., binding that was abolished by a 100-fold excess of TCDF and was not present when unprogrammed lysate was used in place of lysate containing the AHR translation products). In contrast, no specific binding of [^{3}H]TCDD to zfAHR1 was detected under any of these conditions (Fig. 8, A–C). To further explore the ligand-binding specificity of zfAHRs, we examined the ability of these proteins to bind the nonhalogenated compound [^{3}H]BNF, a known ligand of mammalian AHRs. [^{3}H]BNF (10 nM) exhibited a peak of specific binding to the in vitro-expressed human AHR (Fig. 8F), which sedimented at ~10*S* and was displaced by a 100-fold excess of unlabeled BNF (not shown). zfAHR2 exhibited a small but reproducible peak of [^{3}H]BNF-specific binding (Fig. 8E). However, there was very little specific binding of [^{3}H]BNF to in vitro-expressed zfAHR1 (Fig. 8). Because coexpression of zfAHRs and zfARNT2b enhances the interaction with DREs in electrophoretic mobility shift assays (see above), we also performed radioligand binding studies in which zfAHRs and zfARNT2b were expressed individually or together, in the presence of [^{3}H]TCDD. zfAHR1 again failed to exhibit any specific binding of [^{3}H]TCDD, in contrast to zfAHR2, which exhibited strong specific binding whether expressed alone or with zfARNT2b (Fig. 9, A and B).

Screening Assay for zfAHR1 Ligands. The transient transactivation assay was used to investigate the possibility that zfAHR1 and zfAHR2 have differential ligand-binding preferences. COS-7 cells were transfected as described above but exposed to maximal-effect concentrations of other polychlorinated aromatic hydrocarbons (Abnet et al., 1999b). zfAHR2 was active in response to 1,2,3,7,8-pentachlorodibenzo-*p*-dioxin, TCDF, PeCDF, and PCB126, whereas zfAHR1 failed to respond to any of these polychlorinated aromatic hydrocarbons (Fig. 10). To illustrate the extremely low basal luciferase activity of cells transfected to express zfAHR1, the data for zfAHR1 and zfARH2 were plotted on two separate figures. This illustrates that the basal activity of cells expressing zfAHR1 was more than 2 orders of magnitude lower than that of cells expressing zfAHR2. Greater fold induction was observed with cells expressing zfAHR2 (4.4- to 10-fold) when using a luciferase reporter driven by the rainbow trout CYP1A promoter *prt1Aluc* [described previously in Abnet et al. (1999a)] (data not shown). In an effort to screen other potential ligands for zfAHR1, the assay was repeated with maximal-effect concentrations of other known inducers of the AHR pathway (BNF, BaP, DMBA, HxCDD, I3C, 3MC, TCDF, TBDD, and I3AA) (Postlind et al., 1993; Heath-Pagliuso et al., 1998; Abnet et al., 1999b; Seidel et al., 2000; Stephensen et al., 2000; Henry et al., 2001). Luciferase activity was elevated in cells expressing zfAHR2 and exposed to TCDD, BaP, DMBA, HxCDD, 3MC, I3AA, TCDF, TBDD, and I3AA (Fig. 11B). Similar results were obtained in cells transfected with the *prt1Aluc* reporter (data not shown). Surprisingly, BNF exposure actually repressed luciferase activity. The lack of BNF activity in transfection assays with zfAHR2 is consistent with the poor ability of this receptor to bind [^{3}H]BNF noted above and with the inability of this compound to induce CYP1A in a zebrafish cell line or by adult waterborne exposure (Miranda et al., 1993; Collodi et al., 1994). However, dietary or i.p. exposure to BNF has been demonstrated to slightly induce zfCYP1A protein in adult zebrafish (Troxel et al., 1997). This may suggest that exposure route and or metabolism of BNF may be important for induction of zfCYP1A. Again, cells expressing zfAHR1 expressed extremely low luciferase activity independent of whether they were exposed to ligand (Fig. 11A). zfAHR1 was activated slightly by TCDD, 3MC, and I3AA; however, the actual levels of activity were low (near the level of detection of the assay) in comparison with the basal activity of zfAHR2 (Fig. 11). Together, these results demonstrate that a wide range of known AHR ligands activate zfAHR2 but not zfAHR1.

Localization of a zfAHR1 Subdomain Activity. The primary amino acid sequence of zfAHR1 suggests that this

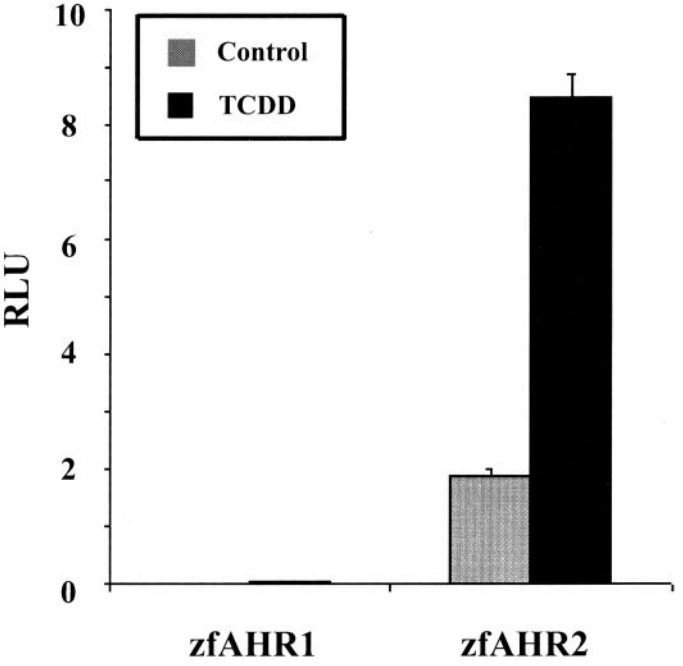

Fig. 6. TCDD-induced transactivation activity of zfAHR1 and zfAHR2 in COS-7 cells. Cells were transiently transfected with expression constructs for either zfAHR1 or zfAHR2 along with zfARNT2b, a β-galactosidase reporter, and an AHR-responsive luciferase expression construct driven by the mouse *cyp1a1* enhancer (*pGudluc1.1*). Twenty-four hours after transfection, cells were exposed to 10 nM TCDD for 20 h followed by luciferase activity analysis. Bars represent relative light units normalized to β-galactosidase activity (mean ± S.E., $n = 3$).

protein is an ortholog of the mammalian AHR; however, zfAHR1 seems to lack functional activities characteristic of the mammalian AHR. In an attempt to dissect the functional domains of zfAHR1, chimeric zfAHRs were generated by exchanging zfAHR1 and zfAHR2 domains (Fig. 12B). All of the chimeric *zfAHR* expression constructs produced proteins of the expected size and were translated with similar efficiency in vitro in rabbit reticulocyte lysates (Fig. 12A). The ability of the chimeric zfAHRs to activate a DRE-driven luciferase reporter was assessed in COS-7 cells by transiently transfecting a *zfAHR* expression construct along with *zfARNT2b* and the *pGudluc1.1* luciferase reporter as described above. zfAHR1 and zfAHR2 responded to TCDD as described previously (Fig. 11B). Knowing that zfAHR1 failed to bind TCDD in a velocity sedimentation assay and only had a very weak interaction with zfARNT2b and the rtDRE in the gel-shift assay, we first exchanged the ligand-binding domains between the zfAHRs. When the ligand-binding domain of zfAHR1 was inserted into zfAHR2 (zfAHR2-1LBD) there was a decrease in basal activity compared with the wild-type zfAHR2, and this chimeric protein failed to respond to TCDD. When the reciprocal chimera zfAHR1-2LBD was examined, the basal luciferase expression was extremely low, like that of the zfAHR1, and this construct also failed to respond to TCDD. These results demonstrate that other domains, in addition to the LBD, contribute to the ultimate lack of transactivation activity of zfAHR1.

Another series of chimeras were constructed by exchanging the LBD and C-terminal domains (chimeras 1-2-2 and 2-1-1) or just the C-terminal domains (chimeras 1-1-2 and 2-2-1). *zfAHR1* transfected cells expressed only 1% of the basal luciferase activity and only 0.4% of the TCDD-induced luciferase activity as cells transfected with *zfAHR2*. Chimera 1-2-2, which contains the bHLH and the PAS-A domain of zfAHR1 and the LBD and C-terminal domain from zfAHR2, displayed repressed basal luciferase activity, only 11.5% of zfAHR2. However chimera 1-2-2 did respond to TCDD with a 13-fold induction. This indicates that the bHLH/PAS-A domains of zfAHR1 are able to function when placed in the context of a functional LBD and transactivation domain. In the chimeric protein containing the bHLH and the PAS-A domain of zfAHR2 and the LBD and C-terminal domain from zfAHR1 (chimera 2-1-1), the basal and TCDD-induced activation of the *pGudluc1.1* reporter was completely lost. This indicates that the LBD and C-terminal domains of zfAHR1 are unable to activate reporter gene activity when fused to functional bHLH and PAS-A domains. Finally, to specifically test the activities of the zfAHR C-terminal domains, the zfAHR1 and zfAHR2 C-terminal domains were exchanged to create chimeras 1-1-2 and 2-2-1. When the zfAHR2 transactivation domain was fused to the bHLH, PAS, and LBD of zfAHR1, this protein (chimera 1-1-2) failed to activate gene expression. This confirms that the LBD of zfAHR1 is nonfunctional. When the zfAHR1 transactivation domain was fused to the bHLH, PAS, and LBD of zfAHR2, this protein (chimera 2-2-1) also failed to respond to TCDD. Taken together, these results are consistent with the hypothesis that the zfAHR1 C-terminal transactivation domain and the LBD are functionally deficient in this transient transfection assay.

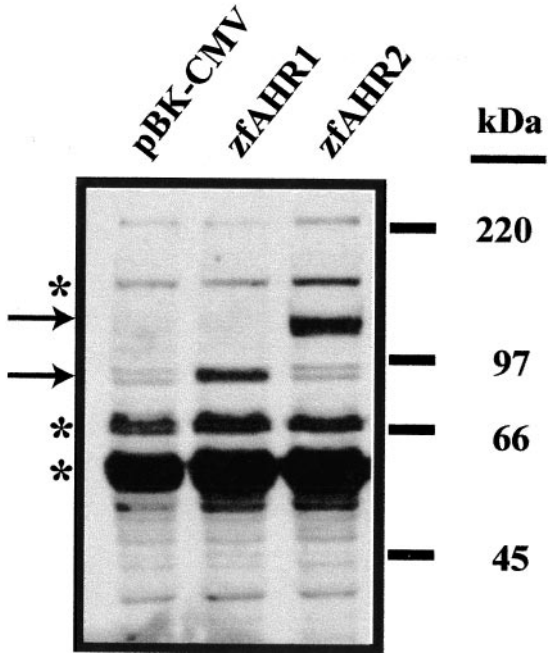

Fig. 7. Western-blot analysis detecting the presence of zfAHR1FLAG and zfAHR2FLAG in COS-7 cell lysate. COS-7 cells were transiently transfected with expression constructs for zfAHR1FLAG, zfAHR2FLAG, or an empty vector (pBKCMV). Lysate was harvested after 30 h. Twenty micrograms of lysate was resolved on an 8% SDS PAGE gel and transferred to nitrocellulose membrane for Western analysis. The membrane was incubated with 2 mg/ml anti-FLAG antibody followed by goat anti-mouse horseradish peroxidase (1:5000). Enhanced chemiluminescence was used to visualize the bands. Arrows indicate the positions of the zfAHRFLAG bands. The asterisk indicates nonspecific bands. Protein molecular mass standards are indicated to the right of the gel.

Discussion

Previously, we have described zfAHR2 and zfARNT2b, functional members of the AHR signal transduction pathway in zebrafish. zfAHR2 was shown to interact with zfARNT2b in a DNA gel-shift assay and functioned in a TCDD-responsive transactivation assay. Here, we have identified another AHR in zebrafish, zfAHR1. Based upon the degree of sequence identity to the mammalian AHRs, this zfAHR has been categorized as a type 1 AHR (Fig. 2). The 805 amino acid zfAHR1 is significantly smaller than the previously described zfAHR2 (1027 aa), with the difference occurring C-terminal to the PAS domain (Fig. 1), but zfAHR1 is similar in size to the murine Ah^{b-1} allele. zfAHR1 shares high sequence similarity with known AHRs in the bHLH, PAS, and ligand-binding domains (Fig. 1). Important motifs such as the NLS and NES sites are conserved in both zebrafish AHRs. However significant sequence divergence occurs in the C terminus of the zfAHRs as has been shown in all reported AHRs. Sequence analysis reveals that neither zfAHR1 nor zfAHR2 contains a Q-rich domain in the C terminus. This Q-rich domain in the mammalian AHR has been shown to be important for transactivation (Kumar et al., 2001). As previously reported (Tanguay et al., 1999), this domain has not been detected in the majority of fish AHRs [with the exception of *F. heteroclitus* AHR1 (Karchner et al., 1999)]. The fact that fish AHRs lacking this domain nevertheless have transactivation activity (Abnet et al., 1999a,b; Tanguay et al., 1999, 2000) indicates that this domain may not be required for functional transactivation in some fish.

In our efforts to establish zebrafish as a model to study

TCDD-mediated toxicity, it was essential to determine which receptor(s) mediates the TCDD-response in zebrafish tissues. Developmental and tissue-specific patterns of expression can provide clues to protein function. Here, we report that zfAHR1 and zfAHR2 mRNAs are expressed early in development, and expression is not significantly altered by TCDD exposure. The in situ localization of components of the AHR signaling has recently been determined for zebrafish embryos and larvae (Andreasen et al., 2002). The early developmental zfAHR2, zfARNT2b, and zfCYP1A expression patterns overlap in some tissues, and zfAHR1 expression was too low for whole-mount studies (Andreasen et al., 2002). In adult tissues, the distribution of zfAHR1 differs drastically from zfAHR2. Whereas zfAHR2 was expressed in all the tissues examined, zfAHR1 was detected in the liver and to a much lesser extent in the heart, kidney, and swimbladder. The zfAHR1 and zfAHR2 mRNA expression pattern is similar to that reported for the two FhAHRs, in that FhAHR2 is widely expressed, whereas FhAHR1 has a restricted tissue distribution (Karchner et al., 1999). However, FhAHR1 and zfAHR1 differ in the specific tissues in which they are expressed. FhAHR1 is particularly abundant in the heart, ovary, and brain (Karchner et al., 1999), whereas zfAHR1 was not detected in the brain and to only a limited extent in the heart. This disparity between zfAHR1 and FhAHR1 expression patterns remains to be explained, but the possibility exists that other AHRs will be identified in these fish species. For zebrafish, the colocalization of zfAHR2- and TCDD-induced expression of zfCYP1A mRNA suggests that zfAHR2, and not zfAHR1, is most probably the AHR involved in TCDD activation of AHR signaling in these tissues. The hallmark signs of TCDD developmental toxicity in zebrafish larvae consist of pericardial and yolk sac edema, reduced blood flow to most peripheral vascular beds, anemia, impaired swimbladder inflation, and impaired lower jaw development. It is significant that many of the tissues involved in these responses to TCDD exposure in zebrafish larvae, namely the heart, blood vessels, kidney, and lower jaw primordia, all express zfAHR2 (Belair et al., 2001; Andreasen et al., 2002; Teraoka et al., 2002). Furthermore, zfAHR2 mRNA was elevated in response to TCDD exposure in the heart and swimbladder of adult zebrafish and in the lower jaw primordia of zebrafish larvae (Teraoka et al., 2002). In contrast, the abundance of zfAHR1 message in zebrafish larvae is so low that it cannot be detected by whole-mount in situ hybridization (Andreasen et al., 2002). It remains a possibility that zfAHR1 may play a specific functional role in development or in the adult liver; however, further research is needed to define this role.

Knowledge of functional properties is important for elucidating the role that each zebrafish AHR may play in TCDD developmental toxicity. In vitro functional studies comparing zfAHR1 and zfAHR2 revealed that the two proteins have very distinct properties. Velocity sedimentation assays reveal that zfAHR2 strongly interacts with TCDD directly in vitro, whereas zfAHR1 does not. zfAHR1 also lacks the abil-

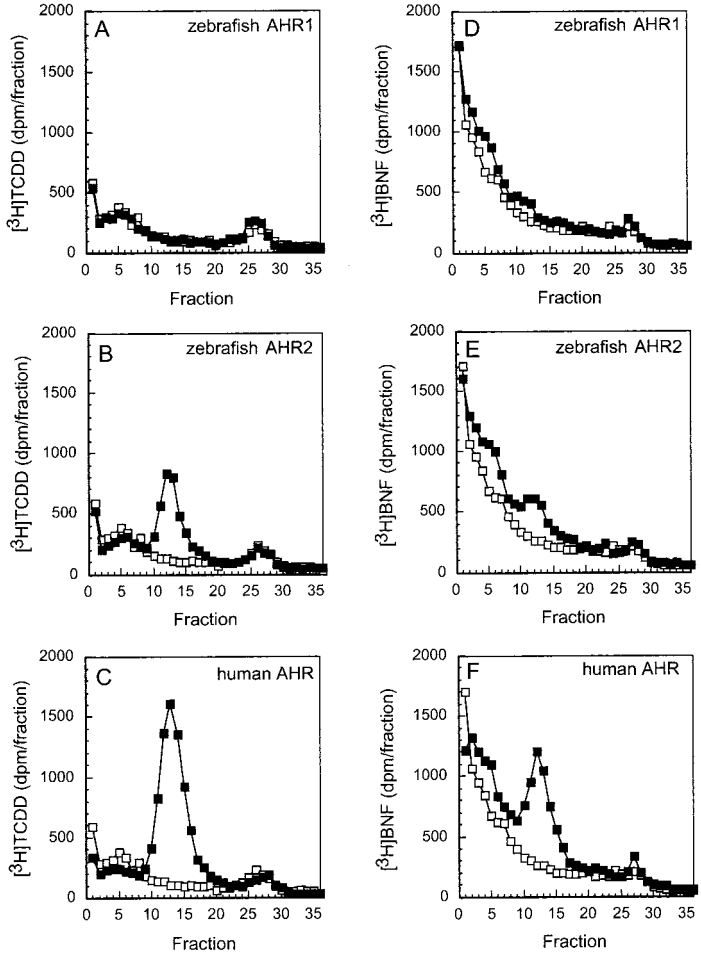

Fig. 8. Analysis of [^{3}H]TCDD- and [^{3}H]BNF-specific binding to in vitro-expressed zfAHR1, zfAHR2, and human AHR. Left, the specific binding of [^{3}H]TCDD to zfAHR1 (A), zfAHR2 (B), and human AHR (C) was analyzed by velocity sedimentation on sucrose gradients using a vertical tube rotor as described under *Materials and Methods*. AHR proteins (■, specific binding; □, nonspecific binding) or zfARNT2 were expressed by in vitro transcription and translation and incubated with 5 nM [^{3}H]TCDD overnight at 4°C before centrifugation. The binding of [^{3}H]TCDD to unprogrammed lysate was indistinguishable from binding to zfARNT2 (not shown). The [^{3}H]TCDD concentration was verified by sampling each tube for total counts. The sedimentation markers [^{14}C]ovalbumin (3.6 *S*) and [^{14}C]catalase (11.3 *S*) eluted at fractions 3 to 4 and 14 to 16, respectively. The peak of [^{3}H]TCDD-specific binding to zfAHR2 and the human AHR represents 39 and 91 fmol of radioligand, respectively. Right, the specific binding of 10 nM [^{3}H]BNF to zfAHR1 (D), zfAHR2 (E), and human AHR (F) was analyzed as described above. The sedimentation markers [^{14}C]ovalbumin (3.6 *S*) and [^{14}C]catalase (11.3 *S*) eluted at fractions 3 to 4 and 14 to 15, respectively. The peak of [^{3}H]BNF-specific binding to zfAHR2 and the human AHR represents 47 and 104 fmol of radioligand, respectively. Each curve represents a single 50-μl TNT reaction. The experiment was repeated several times under various conditions [2–10 nM [^{3}H]TCDD; 10–30 nM [^{3}H]BNF; 2- or 18-h incubation time; low and high salt (0.5 M KCl)], with consistent results.

ity to bind BNF, whereas zfAHR2 has weak BNF binding activity. The lack of significant zfAHR BNF binding in this in vitro assay is consistent with the observation that BNF fails to induce CYP1A in zebrafish liver cell cultures (Miranda et al., 1993). The lack of TCDD or BNF binding by zfAHR1 cannot be explained from differential protein expression because equal amounts of each receptor were used in these experiments. It is possible that the zfAHR1 protein is unable to fold into a ligand-binding conformation in these in vitro experiments, perhaps because it may require an unknown zebrafish protein for proper folding or stability. However to date more than a dozen vertebrate AHRs expressed from cDNAs in vitro have been shown to bind ligand in this assay, so zfAHR1 would be unique in this regard. It is also possible that zfAHR1 exhibits weak interactions with TCDD that are below the limit of detection of this tritium-based binding assay, a conclusion suggested by the gel-shift data (see below). Regardless, the velocity sedimentation data strongly suggest that zfAHR1 lacks the capacity for high-affinity TCDD binding that is characteristic of other vertebrate AHRs. The apparent lack of TCDD binding by zfAHR1 is the first example of a vertebrate AHR that fails to bind TCDD either in vitro or in vivo. FhAHR1, the only other characterized full-length fish AHR1, has been shown to bind TCDD in vitro, illustrating again a difference between zfAHR1 and the FhAHR1 (Karchner et al., 1999). It is worth noting that a common characteristic of the invertebrate AHR-like proteins from *D. melanogaster, C. elegans*, and *Mya arenaria* is their inability to bind TCDD or BNF (Butler et al., 2001). Thus, in its ligand-binding characteristics, zfAHR1 is more similar to invertebrate AHRs than to the vertebrate AHRs.

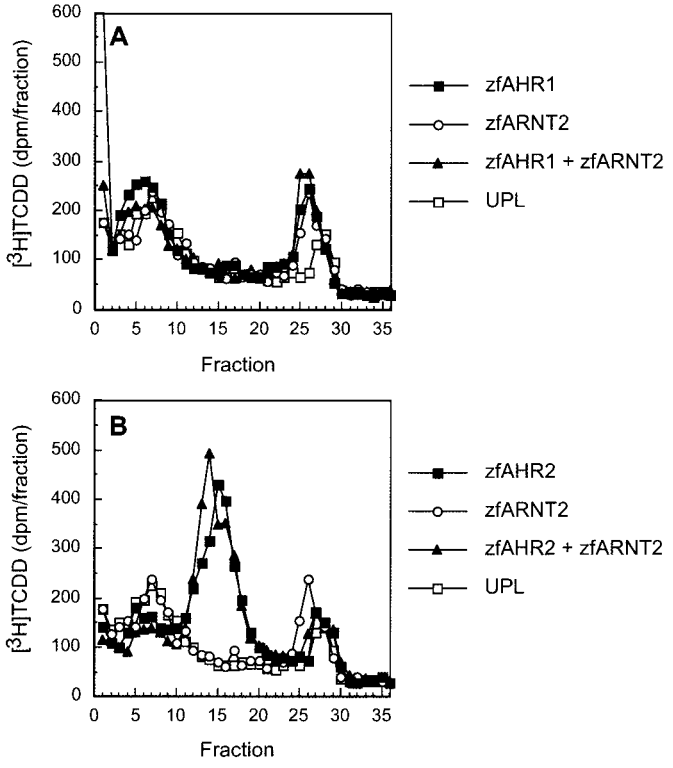

Fig. 9. Analysis of [^{3}H]TCDD-specific binding after coexpression of zfAHR1, zfAHR2, and zfARNT2. zfAHR1 (A) or zfAHR2 (B) was expressed singly or coexpressed with zfARNT2b as described for the DNA binding assays. After in vitro transcription and translation (90 min at 30°C) in the presence of 5 nM [^{3}H]TCDD, reactions were analyzed by velocity sedimentation as described in the legend to Fig. 8.

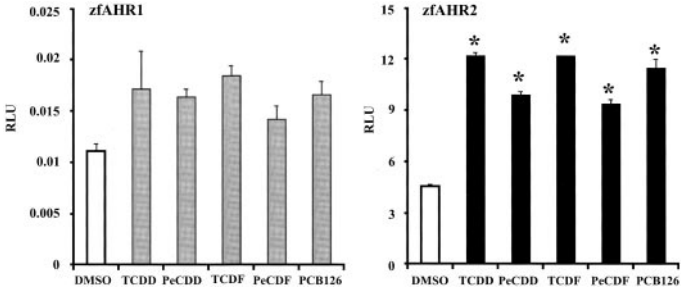

Fig. 10. *trans*-Activation activity of zfAHR1 and zfAHR2 in response to different polychlorinated aromatic hydrocarbons in COS-7 cells. Cells were transiently transfected with expression constructs for either zfAHR1 (A) or zfAHR2 (B) along with zfARNT2b, a β-galactosidase reporter, and an AHR-responsive luciferase expression construct driven by the mouse *cyp1a1* enhancer (*pGudluc1.1*). Twenty-four hours after transfection, cells were exposed to the indicated ligand for 20 h followed by luciferase activity analysis. Exposure concentrations were 10 nM 2,3,7,8-TCDD, 100 nM 1,2,37,8-PcCDD, 100 nM TCDF, 100 nM 2,3,4,7,8-PeCDF, and 1000 nM PCB126. Bars represent the relative light units normalized to the β-galactosidase activity for three replicates treated with DMSO or the indicated aromatic hydrocarbon (mean ± S.E., $n = 3$). ∗ indicates significant difference from DMSO control (Dunnett's test, $p < 0.05$).

Gel-shift assays using in vitro-expressed proteins reveal that zfAHR2 and zfAHR1 can interact with zfARNT2b and bind DREs in a TCDD-dependent manner. However, the zfAHR1/ARNT2b/DRE complex formation was very weak compared with complexes containing zfAHR2 (Fig. 5). This poor DNA binding activity is consistent with the notion of weak TCDD/zfAHR1 binding as suggested by the velocity sedimentation data. As an alternative, TCDD binding may result in a conformation of zfAHR1 that is unable to dimerize with ARNT and bind DNA. Arguing against this is the observation that the zfAHR1 DNA binding domain (PSKRHR) exactly matches the consensus sequence (Swanson and Yang, 1996) and is 100% identical in zfAHR1 and zfAHR2. However, it is known that residues as far away as the PAS

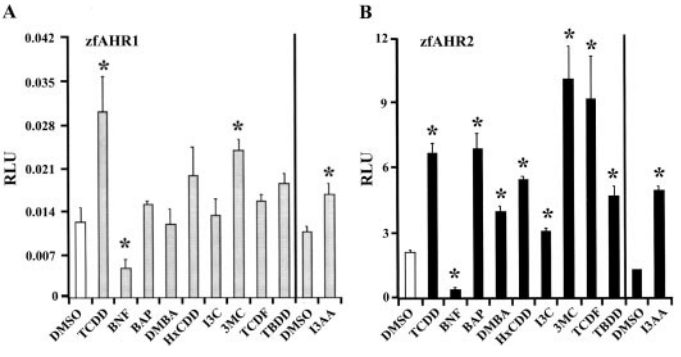

Fig. 11. *trans*-Activation activity of zfAHR1 and zfAHR2 in response to different nontraditional ligands in COS-7 cells. Cells were transiently transfected with expression constructs for either zfAHR1 or zfAHR2 along with zfARNT2b, a β-galactosidase reporter *pGudluc1.1*. Twenty-four hours after transfection, cells were exposed to the indicated ligand for 20 h followed by luciferase activity analysis. The exposure concentrations were 10 nM 2,3,7,8-TCDD, 1 mM BNF, 20 mM BaP, 10 mM DMBA, 10 nM 1,2,3,4,7,8-HxCDD, 1 mM I3C, 1 mM 3MC, 100 nM TCDF, 10 nM TBDD, and 2 mM I3AA. Bars represent the relative light units normalized to the β-galactosidase activity for three replicates treated with 0.5% DMSO or the indicated aromatic hydrocarbon (mean ± S.E., $n = 3$). ∗ indicates significant difference from control ($p < 0.05$, Dunnet's test). Because the I3AA exposure required a higher concentration of vehicle for solubility (DMSO, 1%), statistical significance compared with 1% DMSO control was determined by Student's t test $p < 0.001$).

domain can also alter DNA binding (Sun et al., 1997). It is possible that residues within the bHLH, ARNT dimerization motifs, or C-terminal domains of zfAHR1 may have diverged from the functionally important consensus sequences altering the overall structure and function of the receptor. For instance, zfAHR1 may be less able than other AHRs to form functional complexes with necessary mammalian components present in our assays, leading to lower overall activity. Detailed mutagenesis is required to investigate these possibilities.

Transactivation activity is the culmination of several molecular events in the cell including ligand binding, nuclear translocation, ARNT dimerization, DNA binding, and interaction with basal and specialized transcription factor leading to mRNA synthesis. Here, we show that zfAHR2 and zfAHR1 behaved quite differently in a transient transfection assay (Fig. 6). As seen for other vertebrate AHRs, zfAHR2 had constitutive transactivation activity (i.e., activity seen in the absence of exogenous ligand) in COS-7 cells, and this transactivation activity was enhanced by the addition of TCDD. In contrast, zfAHR1 failed to significantly activate the reporter in the absence of ligand, and addition of TCDD produced only a very slight enhancement, near the limits of detection in this assay. The low reporter gene activity in the presence of zfAHR1 was only 0.2 to 1.0% of that seen with zfAHR2, and this low activity was consistently seen in a number of experiments. Similar transactivation results were obtained using the luciferase reporter gene driven by the rainbow trout *CYP1A* enhancer/promoter, *prt1Aluc* (data not shown) (Abnet et al., 1999a).

Why is zfAHR1 transactivation activity impaired relative to that of zfAHR2? One explanation is that zfAHR1 is unable to efficiently bind TCDD, consistent with our in vitro ligand-binding experiments. It remained a possibility that zfAHR1 evolved to bind a different repertoire of ligands than zfAHR2. By screening the ability of multiple PCAHs and nontraditional ligands to activate zfAHR1 and zfAHR2 in our transient transactivation assay, we found that none of these compounds activated zfAHR1 to an appreciable level. In contrast, multiple ligands activated zfAHR2 (Figs. 10 and 11). Because the tested AHR activators cover a broad range of compounds, including traditional halogenated aromatic and nontraditional ligands, these results suggest that zfAHR1 is unable to bind known AHR ligands. Analysis of the ligand-binding domains of zfAHR1 versus zfAHR2 reveals significant conservation. The domain mapped from mammalian studies, encompassing amino acids 240 to 410, is 65% identical between zfAHR1 and zfAHR2 with a total of 59 amino acid differences. Comparing the zebrafish ligand-binding domains to that of the human AHR, zfAHR1 and zfAHR2 are 68% and 71% identical with the human sequence, respectively. This may be functionally significant, because previous work from different mouse strains indicates that a single amino acid difference can significantly affect ligand binding (Poland et al., 1994).

The lack of zfAHR1 transactivation activity could also result from functional deficits in regions outside of the LBD. For example, the nature of the zfAHR1/zfARNT2b/DRE interaction could be too weak to efficiently affect transcription, the dimerization with other members of the AHR signaling

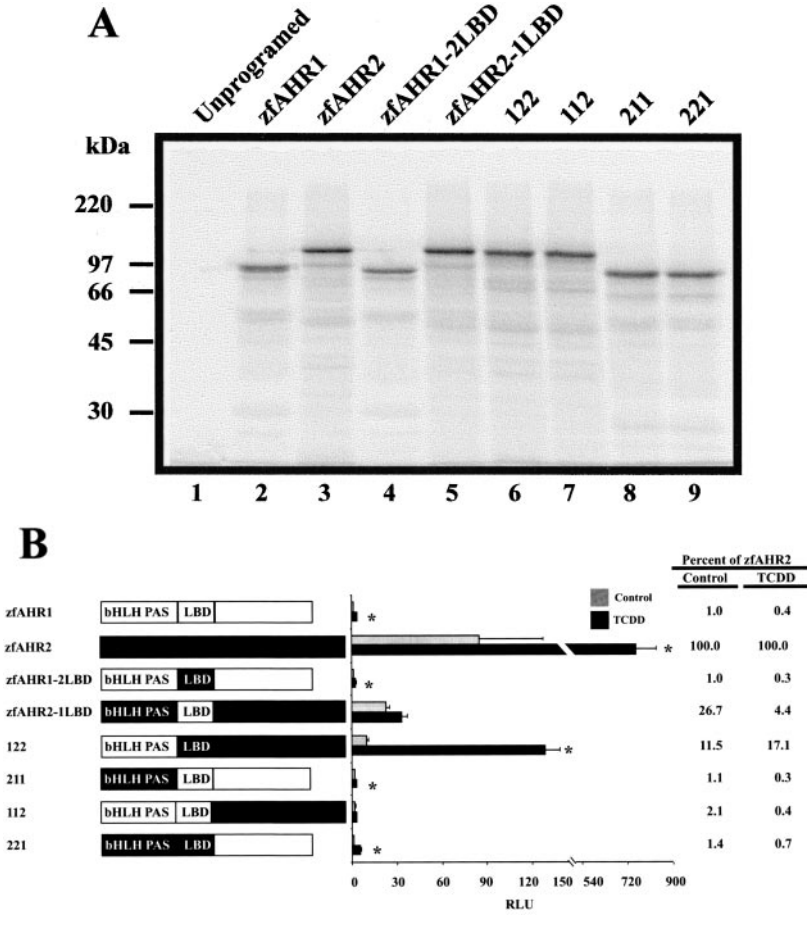

Fig. 12. Transactivation activity of chimeric zfAHRs in COS-7 cells. A, chimeric zfAHR1/zfAHR2 proteins were transcribed and translated in vitro in the presence of [^{35}S]methionine and resolved on an 8% SDS-PAGE gel. A phosphor image of the dried gel is shown; lanes include unprogrammed lysate (lane 1) and in vitro-expressed zfAHR1, zfAHR2, and chimeric zfAHRs (lanes 2–9). B, cells were transiently transfected with expression constructs for the indicated zfAHR construct along with zfARNT2b, a β-galactosidase reporter, and *pGudluc1.1*. Twenty-four hours after transfection, cells were exposed to 10 nM TCDD for 20 h followed by luciferase activity analysis. Bars represent the relative light units normalized to the β-galactosidase activity for DMSO (control) or TCDD (mean ± S.E., $n = 3$). * indicates significant difference from DMSO control (Dunnett's test, $p < 0.05$).

pathway such as HSP90 or AIP could be altered, or perhaps the subcellular localization of zfAHR1 is incorrect. Finally, the transactivation domain of zfAHR1 could also be nonfunctional in its ability to interact with other factors. To begin to investigate these possibilities, chimeric zfAHRs were constructed by swapping domains between the completely functional zfAHR2 and the impotent zfAHR1. By swapping the ligand-binding domains, we demonstrated that that all chimeric constructs containing the zfAHR1 LBD (zfAHR2-1LBD, chimera 2-1-1, and chimera 1-1-2) had low transactivation activity that was only marginally enhanced—if at all—by TCDD. It is important to note, however, that this domain also contains the HSP90 and AIP interaction residues (Meyer and Perdew, 1999); altering the interaction of these accessory proteins with zfAHR1 could inhibit its translocation to the nucleus. In the reciprocal chimera proteins containing the zfAHR2 LBD, appreciable TCDD-responsive activity was only detected in chimera 1-2-2, a protein containing the N-terminal domain from zfAHR1 fused to the LBD and C-terminal domain of zfAHR2. Chimera 2-2-1, containing the N-terminal and ligand-binding domains of zfAHR2 fused to the zfAHR1 C-terminal domain was nearly inactive. In fact, all constructs containing the zfAHR1 C-terminal domain were essentially inactive in this assay, demonstrating that the zfAHR1 C-terminal domain is also nonfunctional. Taken together, the ultimate lack of zfAHR1 transfection activity maps to the C-terminal and LBD domains of the protein.

In summary, a second zebrafish AHR cDNA has been identified and functionally characterized. Although sequence comparisons demonstrate that this novel cDNA represents a zebrafish ortholog of the mammalian AHR, functional studies reveal that zfAHR1 does not act like a traditional TCDD-responsive AHR and is functionally distinct from the only other characterized fish AHR1, FhAHR1 (Karchner et al., 1999). The zfAHR1 protein has properties similar to the AHR-like genes characterized in the invertebrate *D. melanogaster*, *C. elegans*, and *M. arenaria*. Like zfAHR1, the *D. melanogaster*, *C. elegans*, and *M. arenaria* AHR homologs fail to bind TCDD or BNF (Powell-Coffman et al., 1998; Butler et al., 2001). These invertebrate AHR homologs, on the other hand, interact with ARNTs, bind DREs, and are transcriptionally active (Powell-Coffman et al., 1998; Emmons et al., 1999; Butler et al., 2001). Interestingly, the *D. melanogaster* AHR homolog (spineless) interacts with the *D. melanogaster* ARNT homolog (tango) to activate DRE-driven reporters in a ligand-independent manner (Emmons et al., 1999). Little is known about the function of the domains of these invertebrate AHR homologs. Another possibility is that zfAHR1 is functionally similar to the mammalian AHRR. Phylogenetic analysis clearly demonstrates that the zfAHR1 is more similar to the mammalian AHR than any other mammalian PAS protein in GenBank, including mouse and human AHRRs. Moreover, in competitive transactivation assay experiments, zfAHR1 failed to interfere with zfAHR2 transactivation activity (data not shown). Here, we conclude that the region of the protein responsible for the lack of classical AHR-like activity in zfAHR1 is localized to the C-terminal and ligand-binding domains. Taken together, the tissue distribution and functional properties of the proteins suggest that zfAHR1 does not participate in TCDD-mediated toxicity in zebrafish. The lack of TCDD responsiveness of zfAHR1 may partially explain the relative insensitivity of zebrafish to TCDD compared with species such as the rainbow trout that possess at least two functional AHRs. Detailed comparative studies from other fish species are required to test this hypothesis. What is the role for AhR1 in zebrafish? It remains a possibility that zfAHR1 serves as a modifier of the AHR pathway in a ligand-independent manner, or perhaps responds to other ligands during development or in the adult liver.

Acknowledgments

We thank Dorothy Nesbit and Diana G. Franks for excellent technical support and Dr. Marc Ekker (Loeb Health Research Institute, Ottawa, ON, Canada) for assistance in mapping of zfAHR1 and zfAHR2 genes in the LN54 panel.

References

Abnet CC, Tanguay RL, Hahn ME, Heideman W, and Peterson RE (1999a) Two forms of aryl hydrocarbon receptor type 2 in rainbow trout (*Oncorhynchus mykiss*). Evidence for differential expression and enhancer specificity. *J Biol Chem* **274:** 15159–15166.

Abnet CC, Tanguay RL, Heideman W, and Peterson RE (1999b) Transactivation activity of human, zebrafish, and rainbow trout aryl hydrocarbon receptors expressed in COS-7 cells: greater insight into species differences in toxic potency of polychlorinated dibenzo-*p*-dioxin, dibenzofuran and biphenyl congeners. *Toxicol Appl Pharmacol* **159:**41–51.

Andreasen EA, Tanguay RL, Spitsbergen JM, Heideman W, and Peterson RE (2002) Tissue-specific expression of AHR2, ARNT2 and CYP1A in zebrafish larvae: effects of developmental stage and 2,3,7,8-tetrachlorodibenzo-*p*-dioxin exposure. *Toxicol Sci*, in press.

Barbazuk WB, Korf I, Kadavi C, Heyen J, Tate S, Wun E, Bedell JA, McPherson JD, and Johnson SL (2000) The syntenic relationship of the zebrafish and human genomes. *Genome Res* **10:**1351–1358.

Belair CD, Peterson RE, and Heideman W (2001) Disruption of erythropoiesis by dioxin in the zebrafish. *Dev Dyn* **222:**581–594.

Berg P and Pongratz I (2001) Differential usage of nuclear export sequences regulates intracellular localisation of the Dioxin (Ah) receptor. *J Biol Chem* **2:**2.

Butler RA, Kelley ML, Powell WH, Hahn ME, and Van Beneden RJ (2001) An aryl hydrocarbon receptor (AHR) homologue from the soft-shell clam *Mya arenaria*: evidence that invertebrate AHR homologues lack 2,3,7,8-tetrachlorodibenzo-*p*-dioxin and β-naphthoflavone binding. *Gene* **278:**223–234.

Collodi P, Miranda CL, Zhao X, Buhler DR, and Barnes DW (1994) Induction of zebrafish (*Brachydanio rerio*) P450 *in vivo* and in cell culture. *Xenobiotica* **24:**487–493.

Coumailleau P, Poellinger L, Gustafsson JA, and Whitelaw ML (1995) Definition of a minimal domain of the dioxin receptor that is associated with Hsp90 and maintains wild type ligand binding affinity and specificity. *J Biol Chem* **270:** 25291–25300.

Dottavio-Martin D and Ravel JM (1978) Radiolabeling of proteins by reductive alkylation with [14C]formaldehyde and sodium cyanoborohydride. *Anal Biochem* **87:**562–565.

Duncan DM, Burgess EA, and Duncan I (1998) Control of distal antennal identity and tarsal development in *Drosophila* by spineless-aristapedia, a homolog of the mammalian dioxin receptor. *Genes Dev* **12:**1290–1303.

Emmons RB, Duncan D, Estes PA, Kiefel P, Mosher JT, Sonnenfeld M, Ward MP, Duncan I, and Crews ST (1999) The spineless-aristapedia and tango bHLH-PAS proteins interact to control antennal and tarsal development in *Drosophila*. *Development* **126:**3937–3945.

Fukunaga BN, Probst MR, Reisz-Porszasz S, and Hankinson O (1995) Identification of functional domains of the aryl hydrocarbon receptor. *J Biol Chem* **270:**29270–29278.

Garrison PM, Tullis K, Aarts JM, Brouwer A, Giesy JP, and Denison MS (1996) Species-specific recombinant cell lines as bioassay systems for the detection of 2,3,7,8-tetrachlorodibenzo-*p*-dioxin-like chemicals. *Fundam Appl Toxicol* **30:**194–203.

Gasiewicz TA and Neal RA (1979) 2,3,7,8-Tetrachlorodibenzo-*p*-dioxin tissue distribution, excretion and effects on clinical chemical parameters in guinea pigs. *Toxicol Appl Pharmacol* **51:**329–339.

Gu YZ, Hogenesch JB, and Bradfield CA (2000) The PAS superfamily: sensors of environmental and developmental signals. *Annu Rev Pharmacol Toxicol* **40:**519–561.

Hahn ME, Karchner SI, Shapiro MA, and Perera SA (1997) Molecular evolution of two vertebrate aryl hydrocarbon (dioxin) receptors (AHR1 and AHR2) and the PAS family. *Proc Natl Acad Sci USA* **94:**13743–13748.

Hahn ME, Poland A, Glover E, and Stegeman JJ (1994) Photoaffinity labeling of the Ah receptor: phylogenetic survey of diverse vertebrate and invertebrate species. *Arch Biochem Biophys* **310:**218–228.

Heath-Pagliuso S, Rogers WJ, Tullis K, Seidel SD, Cenijn PH, Brouwer A, and Denison MS (1998) Activation of the Ah receptor by tryptophan and tryptophan metabolites. *Biochemistry* **37:**11508–11515.

Henry TR, Nesbit DJ, Heideman W, and Peterson RE (2001) Relative potencies of polychlorinated dibenzo-*p*-dioxin, dibenzofuran and biphenyl congeners to induce cytochrome P4501A mRNA in a zebrafish liver cell line. *Environ Toxicol Chem* **20:**1053–1058.

Hukriede NA, Joly L, Tsang M, Miles J, Tellis P, Epstein JA, Barbazuk WB, Li FN, Paw B, Postlethwait JH et al. (1999) Radiation hybrid mapping of the zebrafish genome. *Proc Natl Acad Sci USA* **96:**9745–9750.
Ikuta T, Eguchi H, Tachibana T, Yoneda Y, and Kawajiri K (1998) Nuclear localization and export signals of the human aryl hydrocarbon receptor. *J Biol Chem* **273:**2895–2904.
Karchner SI, Powell WH, and Hahn ME (1999) Identification and functional characterization of two highly divergent aryl hydrocarbon receptors (AHR1 and AHR2) in the teleost *Fundulus heteroclitus*. Evidence for a novel subfamily of ligand-binding basic helix loop helix-Per-ARNT-Sim (bHLH-PAS) factors. *J Biol Chem* **274:**33814–33824.
Kumar MB, Ramadoss P, Reen RK, Vanden Heuvel JP, and Perdew GH (2001) The Q-rich sub-domain of the human Ah receptor transactivation domain is required for dioxin-mediated transcriptional activity. *J Biol Chem* **276:**42302–42310.
Le Beau MM, Carver LA, Espinosa R III, Schmidt JV, and Bradfield CA (1994) Chromosomal localization of the human AHR locus encoding the structural gene for the Ah receptor to 7p21→p15. *Cytogenet Cell Genet* **66:**172–176.
Lorenzen A and Okey AB (1990) Detection and characterization of [3H]2,3,7,8-tetrachlorodibenzo-*p*-dioxin binding to Ah receptor in a rainbow trout hepatoma cell line. *Toxicol Appl Pharmacol* **106:**53–62.
Meyer BK and Perdew GH (1999) Characterization of the AhR-hsp90-XAP2 core complex and the role of the immunophilin-related protein XAP2 in AhR stabilization. *Biochemistry* **38:**8907–8917.
Mimura J, Yamashita K, Nakamura K, Morita M, Takagi TN, Nakao K, Ema M, Sogawa K, Yasuda M, Katsuki M et al. (1997) Loss of teratogenic response to 2,3,7,8-tetrachlorodibenzo-*p*-dioxin (TCDD) in mice lacking the Ah (dioxin) receptor. *Genes Cells* **2:**645–654.
Miranda CL, Collodi P, Zhao X, Barnes DW, and Buhler DR (1993) Regulation of cytochrome P450 expression in a novel liver cell line from zebrafish (*Brachydanio rerio*). *Arch Biochem Biophys* **305:**320–327.
Poland A, Palen D, and Glover E (1994) Analysis of the four alleles of the murine aryl hydrocarbon receptor. *Mol Pharmacol* **46:**915–921.
Pollenz RS and Necela BM (2000) Analysis of rainbow trout ah receptor proteins *in vitro*. *Toxicologist* **54:**325.
Postlind H, Vu TP, Tukey RH, and Quattrochi LC (1993) Response of human CYP1-luciferase plasmids to 2,3,7,8-tetrachlorodibenzo-*p*-dioxin and polycyclic aromatic hydrocarbons. *Toxicol Appl Pharmacol* **118:**255–262.
Powell-Coffman JA, Bradfield CA, and Wood WB (1998) *Caenorhabditis elegans* orthologs of the aryl hydrocarbon receptor and its heterodimerization partner the aryl hydrocarbon receptor nuclear translocator. *Proc Natl Acad Sci USA* **95:**2844–2849.
Puga A, Barnes SJ, Dalton TP, Chang C, Knudsen ES, and Maier MA (2000) Aromatic hydrocarbon receptor interaction with the retinoblastoma protein potentiates repression of E2F-dependent transcription and cell cycle arrest. *J Biol Chem* **275:**2943–2950.
Roy NK and Wirgin I (1997) Characterization of the aromatic hydrocarbon receptor gene and its expression in Atlantic tomcod. *Arch Biochem Biophys* **344:**373–386.
Schmidt JV and Bradfield CA (1996) Ah receptor signaling pathways. *Annu Rev Cell Dev Biol* **12:**55–89.
Seidel SD, Li V, Winter GM, Rogers WJ, Martinez EI, and Denison MS (2000) Ah receptor-based chemical screening bioassays: application and limitations for the detection of Ah receptor agonists. *Toxicol Sci* **55:**107–115.
Stephensen PU, Bonnesen C, Schaldach C, Andersen O, Bjeldanes LF, and Vang O (2000) *N*-Methoxyindole-3-carbinol is a more efficient inducer of cytochrome P-450 1A1 in cultured cells than indol-3-carbinol. *Nutr Cancer* **36:**112–121.
Sun W, Zhang J, and Hankinson O (1997) A mutation in the aryl hydrocarbon receptor (AHR) in a cultured mammalian cell line identifies a novel region of AHR that affects DNA binding. *J Biol Chem* **272:**31845–31854.
Swanson HI and Yang J (1996) Mapping the protein/DNA contact sites of the Ah receptor and Ah receptor nuclear translocator. *J Biol Chem* **271:**31657–31665.
Swofford DL (1998) PAUP*. Phylogenetic Analysis Using Parsimony (*and Other Methods), Version 4. Sinauer Associates, Sunderland, MA.
Tanguay RL, Abnet CC, Heideman W, and Peterson RE (1999) Cloning and characterization of the zebrafish (*Danio rerio*) aryl hydrocarbon receptor. *Biochim Biophys Acta* **1444:**35–48.
Tanguay RL, Andreasen E, Heideman W, and Peterson RE (2000) Identification and expression of alternatively spliced aryl hydrocarbon nuclear translocator 2 (ARNT2) cDNAs from zebrafish with distinct functions. *Biochim Biophys Acta* **1494:**117–128.
Teraoka H, Dong W, Ogawa S, Tsukiyama S, Okuhara Y, Niiyama M, Ueno N, Peterson RE, and Hiraga T (2002) 2,3,7,8-Tetrachlorodibenzo-*p*-dioxin toxicity in the zebrafish embryo: altered regional blood flow and impaired lower jaw development. *Toxicol Sci* **65:**192–199.
Thompson JD, Gibson TJ, Plewniak F, Jeanmougin F, and Higgins DG (1997) The CLUSTAL_X windows interface: flexible strategies for multiple sequence alignment aided by quality analysis tools. *Nucleic Acids Res* **25:**4876–4882.
Troxel CM, Buhler DR, Hendricks JD, and Bailey GS (1997) CYP1A induction by beta-naphthoflavone, Aroclor 1254 and 2,3,7,8-tetrachlorodibenzo-*p*-dioxin and its influence on aflatoxin B1 metabolism and DNA adduction in zebrafish. *Toxicol Appl Pharmacol* **146:**69–78.
Wang WD, Chen YM, and Hu CH (1998) Detection of Ah receptor and Ah receptor nuclear translocator mRNAs in the oocytes and developing embryos of zebrafish (*Danio rerio*). *Fish Physiol Biochem* **18:**49–57.
Woods IG, Kelly PD, Chu F, Ngo-Hazelett P, Yan YL, Huang H, Postlethwait JH, and Talbot WS (2000) A comparative map of the zebrafish genome. *Genome Res* **10:**1903–1914.

Address correspondence to: Dr. Robert L. Tanguay, Assistant Professor of Molecular Toxicology, University of Colorado Health Sciences Center (UCHSC), Department of Pharmaceutical Sciences, C-238, 4200 East Ninth Avenue, Denver, CO 80262. E-mail:robert.tanguay@uchsc.edu